Table 1. CD20-positive B-cell malignancies treated with rituximab in Nagoya University Hospital

	No. of patients	Disease status at rituximab therapy		Response, RD/PD	Resampling of tumor tissue	CD20 expression, +/±/−
		1st	RD/PD			
DLBCL	51	45	6	13	6	3/1/2
FL	43	26	17	13	7	5/0/2
Nodal marginal zone BCL or MALT	8	6	2	2	2	2/0/0
Burkitt or Burkitt-like	5	5	0	4	2	2/0/0
Mediastinal large B-cell	4	2	2	1	0	0
Intravascular large B-cell	4	4	0	2	1	1/0/0
Mantle cell	4	3	1	1	1	1/0/0
Lymphoplasmacytic	3	3	0	0	0	0
CLL/SLL	2	1	1	0	0	0
Total cases	124	96	28	36	19	14/1/4
Probability (%)				36/124 (29.0)	19/36 (52.5)	5/19 (26.3)

DLBCL indicates diffuse large B-cell lymphoma; FL, follicular lymphoma; BCL, B-cell lymphoma; MALT, mucosa-associated lymphoid tissue; CLL/SLL, clonic lymphocytic leukemia/small lymphocytic lymphoma; 1st, the first treatment; RD/PD, relapse or progression; and +/±/−, positive/decreased/negative.

as the molecular background of the CD20 protein-negative phenotype in cells from those patients.

Methods

Patients

Between February 1988 and November 2006 in Nagoya University Hospital, all 124 patients in this analysis were initially diagnosed with CD20-positive B-cell lymphomas (Table 1) according to the World Health Organization (WHO) classification.[33] All patients were treated with combination chemotherapy with rituximab from September 2001 to December 2006. The median age of the patients was 58 years (range, 16-84 years) at the time of initial rituximab administration. Three patients had received rituximab before September 2001 because of their participation in a previous clinical study. The most recent follow-up date was July 31, 2007, and disease status factors such as relapse, recurrence, and progression were determined by clinical findings and diagnostic imaging using x-ray, computed tomography (CT), magnetic resonance imaging (MRI), and ^{18}F-fluorodeoxyglucose positron emission tomography (FDG-PET). Resampling of tumors at the time of relapse/progression and pathologic analysis of 19 patients was performed. The patients' responses to chemotherapies were evaluated using the International Working Group criteria.[34]

Confirmation of CD20 protein expression by IHC and FCM analyses

These studies were conducted with institutional review board approval from the Nagoya University School of Medicine. After obtaining appropriate informed consent from each patient, in accordance with the Declaration of Helsinki, tumor specimens were harvested from lymph nodes, bone marrow, peripheral blood, or spinal fluid. CD20 protein expression was demonstrated by IHC and/or FCM as indicated previously.[32,35] Briefly, we used mouse anti-CD20 (L26; Dako, Carpinteria, CA), anti-CD10 (Novocastra Laboratories, Newcastle-upon-Tyne, United Kingdom), and anti-CD79a monoclonal antibodies (Dako) for IHC, and mouse anti-CD20 (B2E9; Beckman Coulter, Fullerton, CA) and anti-CD19 (HD37; Dako) monoclonal antibodies for FCM. The CD79a antigen is a pan–B-cell marker that forms a B-cell receptor (BCR) protein complex. The percentages of negative and positive cells from FCM were determined from the data using an isotypic control antibody (mouse IgG1; Beckman Coulter).

Sequence analysis of the *MS4A1* (*CD20*) gene

Genomic DNA from tumor cells was extracted with a QIAamp DNA Blood Mini Kit (QIAGEN, Valencia, CA) and used for further polymerase chain reactions (PCRs). When sufficient tumor cells could not be obtained at diagnosis, genomic DNA from paraffin sections was extracted using the MagneSil Genomic, Fixed Tissue System (Promega, Madison, WI). Genomic DNA PCR was performed using AmpliTaq Gold (Applied Biosystems, Foster City, CA) to acquire fragments of the coding sequences of exons 3 to 8 of the *MS4A1* (*CD20*) gene. The following primers were designed from the appropriate intron sequences to achieve the coding sequences: exon 3-upper (U), 5′-GCT CTT CCT AAA CAA CCC CT-3′; exon 3-lower (L), 5′-CAT GGG ATG GAA GGC AAC TGA C-3′; exon 4-U, 5′-TGC TGC CTC TGT TCT CTC CC-3′; exon 4-L, 5′-CTG CAC CAT TTC CCA AAT GGC T-3′; exon 5-U, 5′-CTC CAT CTC CCC CAC CTC TC-3′; exon 5-L, 5′-GGT ACT TCT CTG ACA TGT GGG A-3′; exon 6-U, 5′-TGG AAT TCC CTC CCA GAT TAT G-3′; exon 6-L, 5′-CCT GGA GAG AAA TCC AAT CTC A-3′; exon 7-U, 5′-GTC TCC TGT ACT AGC AGT TC-3′; exon 7-L, GGC TAC TAC TTA CAG ATT TGG G-3′; exon 8-U, 5′-TGG TCA ATG TCT GCT GCC CT-3′; and exon 8-L, 5′-GCG TAT GTG CAG AGT ACC TCA AG-3′. Amplified fragments were cloned into a pGEM-T Easy Vector (Promega) and were sequenced using a DNA auto sequencer (ABI PRISM 310; Applied Biosystems). PCR fragments that contained each exon sequence were cloned into the pGEM-T vector, and at least 10 clones were sequenced. If a mutation was observed in 2 different clones, we verified that the sequence reflected a mutation in the tumor rather than a PCR error.

RNA extraction and reverse-transcription–polymerase chain reaction

A blood RNA extraction kit (QIAGEN) was used to isolate total RNA from tumor cells. cDNA was prepared as reported previously.[36] For reverse-transcription–polymerase chain reaction (RT-PCR) analyses of CD10, CD19, CD20, and β-actin, the following primers were designed: CD10-U, 5′-TTG TCC TGC TCC TCA CCA TC-3′; CD10-L, 5′-GTT CTC CAC CTC TGC TAT CA-3′; CD19-U, 5′-GAA GAG GGA GAT AAC GCT GT-3′; CD19-L, 5′-CTG CCC TCC ACA TTG ACT G-3′; CD20-U, 5′-ATG AAA GGC CCT ATT GCT ATG-3′; CD20-L, 5′-GCT GGT TCA CAG TTG TAT ATG-3′; β-actin-U, 5′-TCA CTC AAG ATC CTC A-3′; and β-actin-L, 5′-TTC GTG GAT GCC ACA GGA C-3′. Semiquantitative RT-PCR with AmpliTaq Gold was performed as described previously.[32] Quantitative RT-PCR was carried out using TaqMan PCR (ABI PRISM 7000; Applied Biosystems) as previously described.[32,36]

Immunoblot analysis

Cells (~5 × 10^5) were lysed in 100 μL lysis buffer (50 mM tris(hydroxymethyl)aminomethane [Tris]-HCl [pH 8.0], 1.5 mM $MgCl_2$, 1 mM ethylene glycol-bis(β-aminoethyl ester)-*N,N,N′,N′*-tetraacetic acid [EGTA], 5 mM KCl, 10% glycerol, 0.5% Nonidet P-40 [NP-40], 300 mM NaCl, 0.2 mM phenylmethylsulfonyl fluoride [PMSF], 1 mM dithiothreitol [DTT], and a Complete Mini protease inhibitor tablet [Roche Applied Science, Indianapolis, IN]). After centrifugation at 10 000*g* for 10 minutes, the supernatants were placed in new tubes and 100 μL of 2× sodium dodecyl sulfate (SDS) sample buffer was added. After boiling for 5 minutes, samples were

Table 2. CD20-negative RD/PD after treatment with rituximab-containing combination chemotherapy

UPN	Age/ sex	Diagnosis on admission	Status	Chemo Regimen	Total ritux	Duration until CD20−	Diagnosis (RD/PD)	Patho source	CD20 expression				Survival after CD20−
									FCM	IHC	RT	CDS mutation	
1	65/M	DLBCL	2 rel	R-salvage	8	2M	DLBCL	BM	−	−	N.A.	S97F [2/16]	6M†
2	37/ F	DLBCL	1 diag	R-CHOP	8	9M	DLBCL	BM	±*	±†	N.A.	V247I [2/10]	4M†
3	75/M	DLBCL	1 diag	R-CHOP	7	10M	DLBCL	BM, CF	−	−	↓	WT	11M†
4	42/M	FL G1	2 rel	R-CHOP	4	23M	DLBCL	BM	−	−	↓	WT	11M†
5	52/M	FL G2	3 rel	R-cMOPP	14	81M	DLBCL	BM, LN‡	−	−	↓	WT	8M†

Status indicates disease status of those patients at the first treatment with rituximab; rel, relapse; duration until CD20−, duration (in months) until CD20− relapse or PD from the first rituximab treatment; total ritux, total times of rituximab treatment; patho source, sources of tumor tissues for pathologic analysis; BM, bone marrow; CF, cerebral fluid; LN, lymph node; RT, RT-PCR; N.A., not available; ↓, down-regulated; CDS, coding sequences; and survival after CD20−, duration from CD20-negative change until death.

*19% of tumor cells were $CD20^+$.

†30% of tumor cells showed $CD20^+$.

‡Lymph node sample obtained at autopsy.

separated by SDS–polyacrylamide gel electrophoresis (PAGE). Immunoblotting was carried out as described previously[32,37] using goat polyclonal anti-CD20 antibody (Santa Cruz Biotechnology, Santa Cruz, CA) and rabbit polyclonal anti-actin antibody (Santa Cruz Biotechnology).

Treatment of RRBL1 cells and primary lymphoma cells with the epigenetic drug 5-aza-2′-deoxycytidine

RRBL1[32] and primary lymphoma cells (5×10^5) were cultured in 6-well dishes in RPMI 1640 medium containing 10% fetal bovine serum (FBS) for 24 hours with or without 5-aza-2′-deoxycytidine (5-Aza; Sigma-Aldrich, St Louis, MO) at a final concentration of 100 mM. The cells were then washed twice with RPMI 1640 medium containing 10% FBS, and incubated for more than 2 days in the same medium without 5-Aza. Cells were harvested and used for total RNA and protein extraction.

Antibody-dependent cell-mediated cytotoxicity assay in vitro

Antibody-dependent cell-mediated cytotoxicity (ADCC) activity was analyzed by an in vitro chromium-51 (^{51}Cr) release assay. Target cells (RRBL1, Daudi, DHL10) were cultured in appropriate medium supplemented with 10% to 20% FBS. Each cell line (2.0×10^5 cells) was labeled with 100 μCI (3.7 MBq) of $Na_2{}^{51}CrO_4$ (PerkinElmer Japan, Tokyo, Japan) at 37°C for 1 hour. Human peripheral blood mononuclear cells (PBMC), which were obtained from a healthy donor, were prepared as effector cells of the cell-mediated cytotoxicity assay. ^{51}Cr-labeled target cells were divided into aliquots in 96-well plates (10^4 cells/well). Effector PBMC cells (5×10^5 cells/well) were then added to each well in the presence or absence of rituximab (0 to 31.25 μg/mL) and incubated for 4 hours at 37°C. Supernatants were obtained after a brief centrifugation and measured on a γ-ray counter (PerkinElmer). ^{51}Cr-labeled target cells without antibodies were lysed completely by NP-40 (2% final concentration) and used as a positive control (the maximal ^{51}Cr release). The percentage of lysed cells was calculated using the following formula: % cell lysis = [(experimental release (cpm) − background (cpm)/(maximal release (cpm) − background (cpm))] × 100%, where cpm indicates counts per minute.

Results

CD20-negative phenotypic change after treatment with rituximab

A total of 124 patients with CD20-positive B-cell malignancies were treated with rituximab-combined chemotherapy from September 2001 to December 2006 (Table 1). All patients were diagnosed with CD20-positive B-cell lymphomas by IHC and/or FCM analyses using their tumor tissue specimens. Thirty-six patients (29.0%) showed relapse and progression (response; relapse/progression of disease [RD/PD] in Table 1) of their disease after or during chemotherapies with rituximab. Tumor cells from 19 of these 36 patients (52.8%) were resampled at the time of RD/PD, and CD20 protein expression was analyzed by IHC and/or FCM. CD20 protein expression was not detected or was significantly decreased in 5 patients (DLBCL, 3 patients; FL, 2 patients). Therefore, in 26.3% of patients whose tumor cells were resampled at the time of RD/PD, a CD20-negative phenotypic transformation after rituximab treatment was observed.

Clinical and laboratory features of patients with a CD20-negative phenotypic change

The clinical features of the 5 patients with a CD20-negative phenotypic change after rituximab treatment are shown in Table 2. Initially, 3 patients were diagnosed with DLBCL and 2 patients were diagnosed with FL. They were treated with chemotherapy with rituximab (375 mg/m^2) repeatedly until a CD20-negative phenotypic change was observed. Four to 14 cycles of rituximab were administered. These 5 patients showed relapse or progression from 2 to 81 months after their first treatment with rituximab. Histologic transformation from FL was observed in 2 patients, resulting in all 5 patients being diagnosed histologically as DLBCL at the time of RD/PD. Tumor cell infiltration into the bone marrow was observed in all 5 patients. A CD20 protein-negative phenotype was confirmed by IHC (Figure 1) and FCM in all 5 cases. In 3 patients, mRNA from tumor tissues was available, and CD20 mRNA expression was faintly observed using RT-PCR. Although all 5 patients received salvage chemotherapy without rituximab, they all died from disease progression within 11 months of the confirmation of CD20-negative transformation. The clinical outcomes of these patients who showed RD/PD after treatment with rituximab-containing chemotherapy are shown in Table 3. The 5 patients with CD20-negative RD/PD tended to have a shorter survival time than with CD20-positive RD/PD (100% vs 35.7% died). However, statistical significance could not be determined because of the variable disease status of each patient, including different backgrounds, salvage chemotherapies, and other factors. More patients must be studied to further analyze this apparent trend.

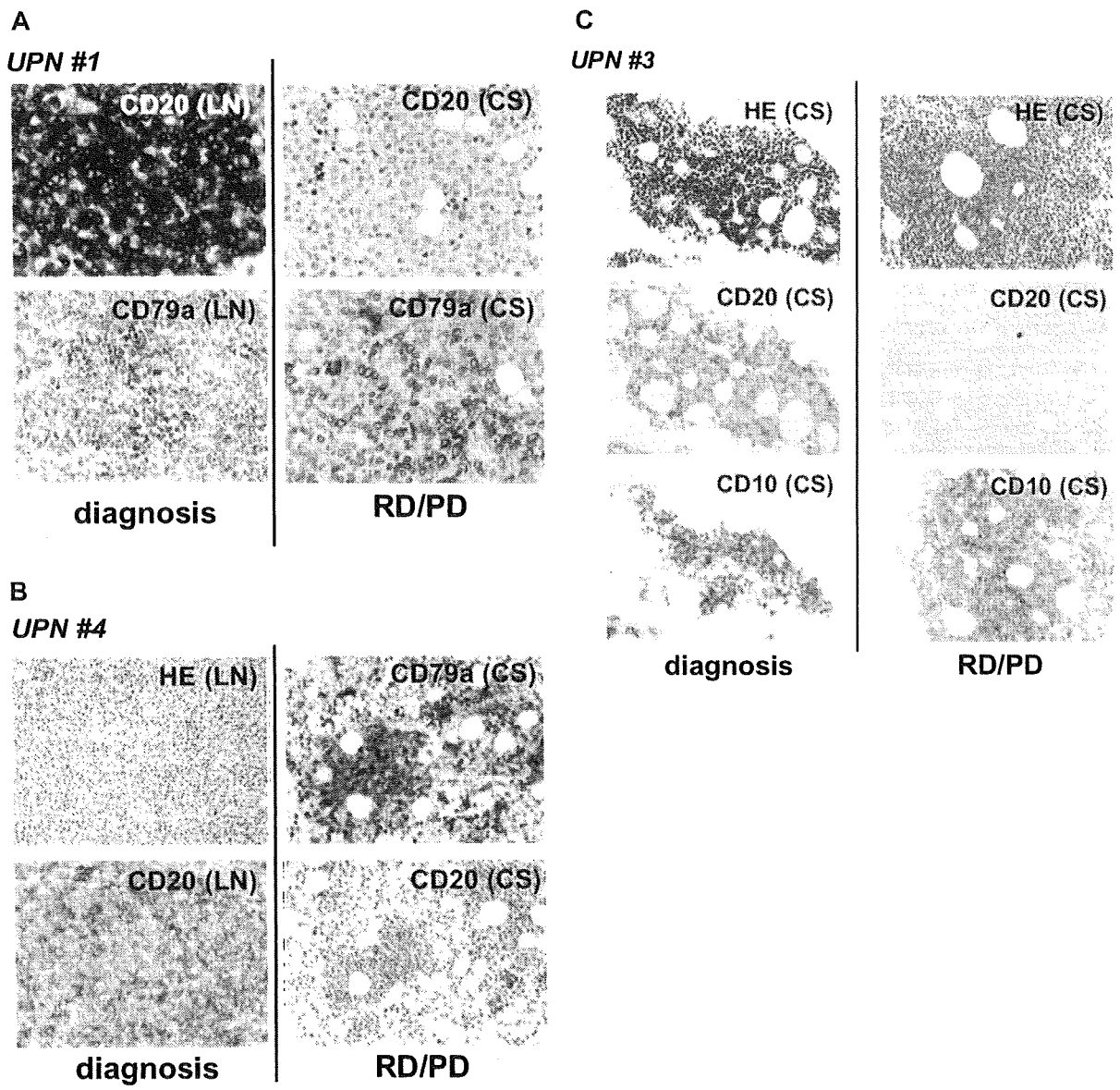

Figure 1. CD20 protein–negative phenotypic changes in CD20-positive B-cell lymphoma patients after treatment with rituximab-containing chemotherapy. Tissue samples (LN, lymph nodes; CS, bone marrow clot section) obtained from UPNs 1 (A), 4 (B), and 3 (C) in Table 2 were analyzed by IHC using anti-CD20, anti-CD79a, and anti-CD10 antibodies. Anti-CD79a antibody was used for detection of B cells. Note that CD20 was positive at the time of initial diagnosis in these patients, and that the CD20-negative phenotypic change was observed during the relapse/progression period. Original magnifications, ×400 (A) and ×200 (B,C) (Olympus BX51TF microscope, Olympus, Tokyo, Japan, and Nikon DS-Fi1 camera, Nikon, Tokyo, Japan). HE indicates hematoxylin and eosin staining; and RD/PD, relapse/progression of disease.

Table 3. Response against salvage chemotherapies for the 36 patients who showed relapse or PD after rituximab-containing chemotherapies.

	CD20 expression		
Response	–	+	N.D.
CR	0	5	3
PR	0	1	3
SD	0	1	1
RD/PD	0	2	2
Death	5	5	8
Total cases	5	14	17

These outcomes were evaluated in July, 2007.

CR indicates complete remisson; PR, partial response; SD, stable disease; RD/PD, relapse/progression; and N.D., Not determined.

Genetic abnormalities in the *CD20* gene

Genomic DNA mutations in the coding sequence (CDS) of the *CD20* gene, also known as the *MS4A1* gene, were also analyzed in the 5 patients. If the mutations were located in specific domains that are recognized by anti-CD20 antibodies including rituximab, those mutations might be related to resistance to rituximab and/or the CD20-negative phenotype. As indicated in Table 2, the change in serine 97 to phenylalanine (S97F; TCC → TTC) in unique patient number (UPN) 1 and valine 247 to isoleucine (V247I; GTT → ATT) in UPN 2 were confirmed in 2 clones each of 16 and 10 clones, respectively. In the other 3 cases, no genetic mutations in the *MS4A1* CDS were detected. Chromosomal analysis by G-banding was also performed using tumor cells obtained from each patient in both the initial diagnosis (CD20-positive) and at the time of RD/PD

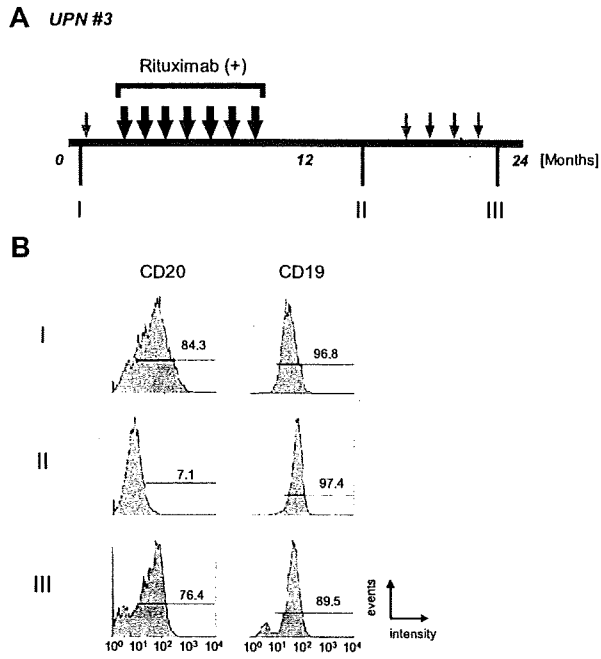

Figure 2. Alteration of CD20 protein expression on B-cell lymphoma cells during disease progression. (A) The clinical course of UPN 3 is depicted briefly. Large black arrows and smaller gray arrows indicate one course of combination chemotherapy with or without rituximab, respectively. Rituximab (375 mg/m^2 each) was administered 7 times. During the patient's 24-month clinical course, tumor cells were harvested at stages I, II, and III from lymph nodes, bone marrow, peripheral blood, and/or cerebral fluid. (B) FCM analysis using anti-CD20 and anti-CD19 antibodies was carried out using tumor cells from peripheral blood. Positive cells are shown in the black lines, and the percentage of positive cells is shown. Note that CD20 expression was observed at the initial diagnosis (I, 84.3%), and that the expression then diminished after treatment with chemotherapy with rituximab (II, 7.1%). Interestingly, CD20 protein expression was observed again at the terminal stage after several chemotherapy treatments without rituximab (III, 76.4%). On the other hand, CD19 expression level was stable throughout the clinical course.

(CD20-negative; Table S1, available on the *Blood* website; see the Supplemental Materials link at the top of the online article). Chromosomal abnormalities involving 11q12 containing the *MS4A1* gene were not observed.

Alteration of CD20 protein and mRNA expression levels after treatment with rituximab

As shown in Figure 1, CD20 protein expression by IHC analysis is altered after chemotherapy with rituximab. The clinical course of UPN 3 is depicted briefly in Figure 2A. FCM analyses using appropriate lymphoma tissues from lymph nodes, peripheral blood, bone marrow, and/or cerebral fluid were performed at admission (I), upon relapse after treatment with rituximab-containing combination chemotherapy (II), and at the end stage of disease after salvage chemotherapy without rituximab (III). The results of FCM analysis using peripheral blood, which contains lymphoma cells, are shown in Figure 2B. Interestingly, CD20 protein expression recognized by FCM analysis was significantly diminished at stage II, but was reversed at stage III. At stage II, CD20-negative lymphoma cell infiltration into the cerebral fluid was also confirmed by FCM analysis (data not shown). On the other hand, CD19 expression, which is also present on B-cell lymphoma cells, was detected constantly throughout the clinical course (Figure 2B right column). Semiquantitative RT-PCR (Figure 3A) and quantitative RT-PCR (Figure 3B) show that the mRNA expression level of *CD20* was significantly altered in each stage. CD20 mRNA expression was faintly observed at stage II (Figure 3B column 4) when CD20 protein expression was barely detectable with FCM (Figure 2B) and IHC (Figure 1C). In UPN 4, CD20 mRNA expression levels were determined by RT-PCR using tumor samples obtained before and after treatment with rituximab-containing chemotherapy (Figure 3C,D). Similar to UPN 3, CD20 mRNA expression was significantly decreased, and no protein expression was detected with IHC (Figure 1B). These findings suggest that CD20 protein expression is mainly regulated at the transcriptional level, and that the expression may be down-regulated in patients who show CD20-negative transformation after treatment with rituximab.

Epigenetic regulation of *CD20* gene expression after treatment with rituximab

These findings suggest that CD20 expression is partly epigenetically regulated by factors such as rituximab treatment surrounding tumor cells, or that CD20-negative tumor cells are able to grow selectively during rituximab treatment. If the CD20-negative B cells still possess the capability to express CD20 protein, we hypothesized that some epigenetic drugs[38,39] may be able to stimulate the *CD20* transcription. First, we examined *CD20* transcription after treatment with 5-Aza using primary tumor cells derived from cerebral fluid of UPN 3 at stage II in Figure 2A, which

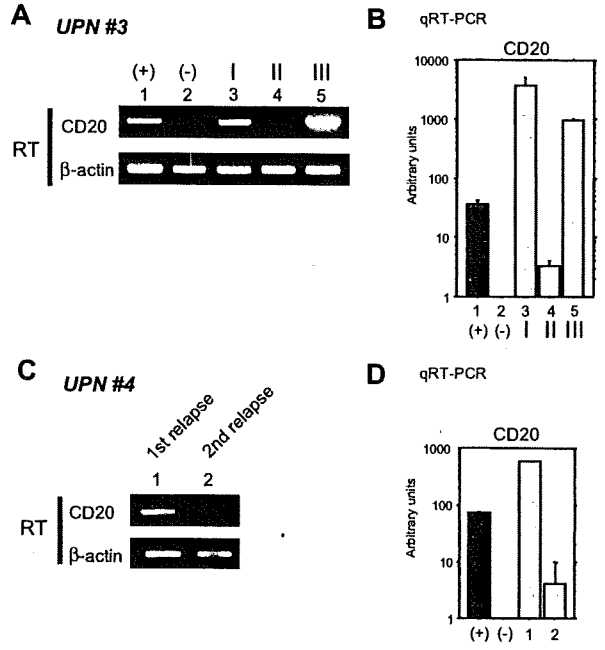

Figure 3. Alteration of CD20 mRNA expression in B-cell lymphoma cells during the clinical course. (A) RT-PCR (RT) was performed using total RNA from the same tumor cells as in Figure 2B (UPN 3 in Table 2). As positive and negative controls, total RNA from Raji and 293T cells was used (lanes 1 and 2), respectively. I, II, and III (lanes 3-5) correspond to the clinical stages depicted in Figure 2A. (B) Quantitative RT-PCR was performed using the same RNA as in panel A. Arbitrary units of CD20 mRNA expression are indicated in the vertical axis. Note that faint expression of CD20 mRNA could be seen at stage II (column 4) despite a loss of CD20 surface protein expression as shown in Figure 2B. (C) CD20 mRNA expression in the lymphoma cells of UPN 4 (Table 2) was also analyzed. Tumor cells were derived from cerebral fluid at the first relapse after chemotherapy without rituximab (lane 1). Although complete remission was obtained after using rituximab-containing salvage chemotherapy, a second relapse occurred. Tumor cells were once again harvested from this patient's cerebral fluid and analyzed (lane 2). (D) Quantitative RT-PCR was also performed using the same RNA as in (C). Note that CD20 mRNA expression was significantly diminished but could still be observed. In these cells, CD20 protein expression was undetectable using FCM or IHC as indicated in Table 2. Positive and negative controls derived from Raji and 293T cells are indicated by + and −, respectively.

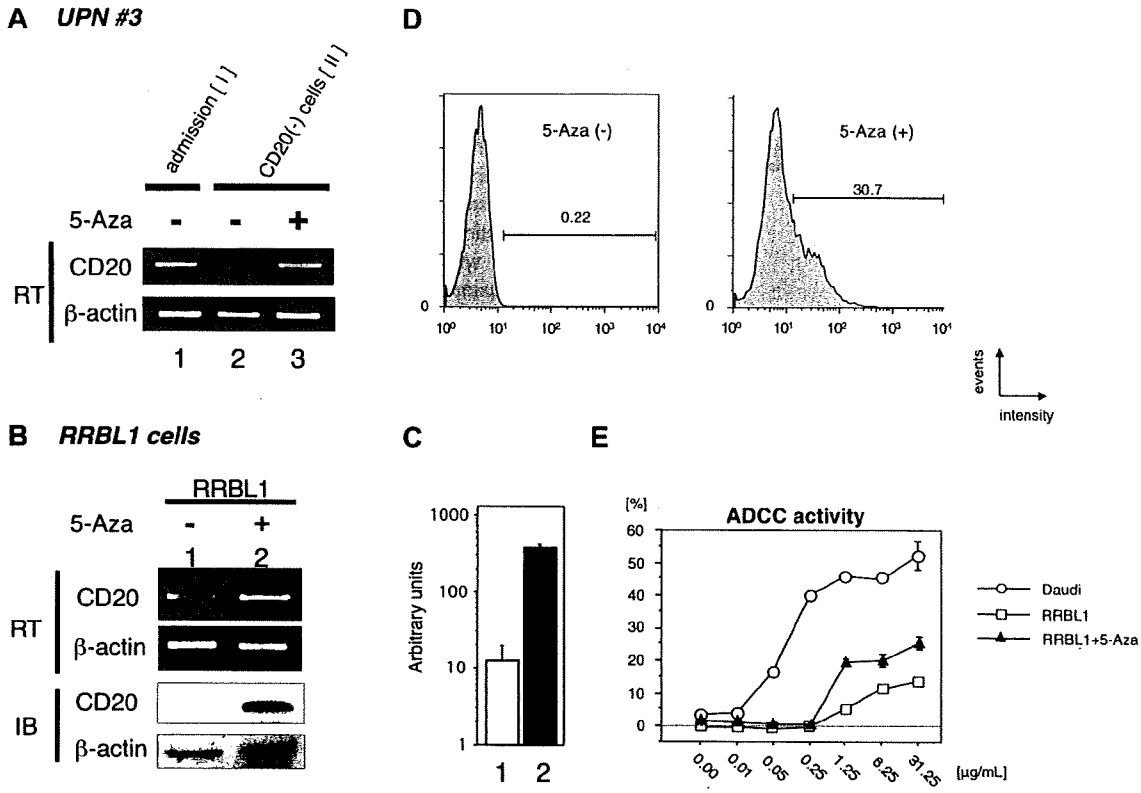

Figure 4. Restoration of CD20 mRNA and protein expression by treatment with the DNA methyltransferase inhibitor 5-Aza. (A) Primary B-cell lymphoma cells, which showed a CD20 protein-negative phenotype from UPN 3, were incubated with or without 5-Aza. Total RNA was prepared, and semiquantitative RT-PCR was performed. Restoration of CD20 mRNA expression after treatment with 5-Aza was observed in lane 3. As a positive control, tumor cells obtained at the initial diagnosis of that same patient were used in lane 1. (B) The CD20 protein-negative B-cell lymphoma cell line RRBL1,[32] which was derived from UPN 5 in Table 2, was incubated in culture medium with or without 5-Aza. After preparation of total RNA and whole-cell lysates from these cells, semiquantitative RT-PCR and immunoblotting (IB) were performed. Up-regulation of CD20 mRNA and protein expression was observed as shown in lane 2. (C) Quantitative RT-PCR was performed using the same mRNA as in (B). We observed an up-regulation of more than 10-fold in CD20 mRNA after treatment with 5-Aza (column 2). (D) RRBL1 cells were treated with 5-Aza under the same conditions as in (B), and FCM analysis using anti-CD20 antibody was performed. After treatment with 5-Aza, 30.7% of RRBL1 cells showed a CD20-positive phenotype. Positive cells are shown with black lines, and the percentage of positive cells is also shown. (E) In vitro ADCC analysis using the ^{51}Cr-release assay. Cells from the CD20-positive B-cell lymphoma/leukemia cell lines Daudi and RRBL1 treated with or without 5-Aza were used for this assay. In Daudi cells (○), but not in RRBL1 cells (□), cytotoxic activity was observed in the presence of rituximab in a dose-dependent manner. Partial restoration of rituximab sensitivity in RRBL1 cells was observed after treatment with 5-Aza (▲). Error bars indicate plus or minus 1 standard deviation.

showed a CD20-negative phenotype. As a CD20-positive control, lymphoma cells at the initial diagnosis from the same patient were used (Figure 4A lane 1). After treatment with 5-Aza in vitro, significant stimulation of CD20 expression was observed (Figure 4 lane 3).

Previously, we established the CD20-negative B-cell lymphoma cell line RRBL1,[32] which was derived from CD20-negative tumor cells in peripheral blood from a patient (UPN 5 in Table 2). Next, we performed the same assay using these cells (Figure 4B), and we were able to show up-regulation of CD20 mRNA expression (Figure 4B,C). CD20 protein expression induction was also confirmed by immunoblotting (Figures 4B, IB). Thus, these data, showing that CD20 expression could be stimulated within a few days, suggested that CD20 expression is down-regulated by epigenetic mechanisms.

Restoration of rituximab sensitivity in CD20-negative cells after treatment with 5-Aza in vitro

From these findings, we hypothesized that rituximab sensitivity would be restored if we could stimulate CD20 protein expression on the surface of CD20-negative transformed lymphoma cells. To test this hypothesis, we performed FCM analysis and an in vitro ADCC assay using RRBL1 cells with or without 5-Aza treatment. As shown in Figure 4D, CD20 protein expression was induced on the surface of 30.7% of RRBL1 cells after treatment with 5-Aza. Using these cells with or without 5-Aza treatment, an in vitro ^{51}Cr-release assay was performed to confirm ADCC activity induced by rituximab (Figure 4E). Daudi cells were used as CD20-positive rituximab-sensitive control cells. In the presence of rituximab, cell death was observed in a dose-dependent manner in Daudi cells. In contrast, the percentage of RRBL1 cells undergoing cell death was significantly lower despite the high concentration of rituximab. RRBL1 cells treated with 5-Aza showed partial rituximab sensitivity compared with RRBL1 cells not treated with 5-Aza. These experiments were done in triplicate and repeated at least 3 times, with similar results. These data suggest that CD20 expression and rituximab sensitivity could be restored in some cases using epigenetic drug treatment even when CD20-negative transformation results from rituximab treatment. Further experiments using patients' primary samples and an in vivo system will be required to further explore this idea.

Discussion

Rituximab is a clinically important antitumor monoclonal antibody targeting the CD20 surface antigen expressed on B-cell malignancies. However, its effectiveness is sometimes unsatisfactory since a significant percentage of patients treated with rituximab-containing

chemotherapy showed relapse or progression.[3,6,40] In this report, we also estimated that RD/PD after treatment with rituximab was observed in almost 30% of B-cell lymphoma patients after treatment with combination chemotherapies with rituximab. Importantly, not all patients who show RD/PD demonstrate resistance to rituximab. In fact, some patients were sensitive to retreatment with rituximab-containing salvage chemotherapies (data not shown). We may need to define "rituximab resistance" more carefully by monitoring each patient's clinical course.

A CD20-negative phenotypic change was observed in 26.3% of patients for whom tumor resampling (rebiopsy) was carried out (Table 1). We generally perform rebiopsies when tumor progression becomes very aggressive or when the manner of tumor expansion significantly changes during clinical observation. If we had carried out resampling on every RD/PD patient, the percentage of patients with CD20-negative transformations may have been much lower. Thus, examination of more patients will be critical. One important observation about the CD20-negative phenotypic change is that all 5 patients died from their disease progression within 1 year after showing a CD20-negative transformation (Tables 2,3). This observation may indicate that a loss of CD20 expression is partly related to poor prognosis. In our study, however, patients' backgrounds varied (eg, age, sex, pathologic findings, chemotherapy regimens, and organ function). A larger patient sample is warranted to determine the significance of the loss of CD20 expression.

It is noteworthy that CD20 mRNA expression was confirmed by RT-PCR even in those tumor cells that showed a CD20 protein-negative phenotype using IHC, FCM, and immunoblotting (Figure 3). In one case (Figure 3, UPN 3), expression of CD20 mRNA and protein were observed again after salvage chemotherapy without rituximab. Clonal evolution may be one reason for the alteration of CD20 mRNA and protein expression patterns in the same patient either with or without rituximab. However, our finding of the restoration of CD20 mRNA and protein expression within 3 days after treatment with 5-Aza (Figure 4) may instead support the idea that expression is regulated by epigenetic mechanisms, rather than by the alteration of several tumor clones.

We cannot exclude the possibility that genetic alteration in tumor cells that affects the expression of transcription factors PU.1, Pip, and Oct2, which are thought to be critical for *MS4A1* (*CD20*) gene expression,[41] may contribute to the aberrant *CD20* transcriptional regulation. We analyzed the methylation status of cytosine guanine dinucleotides (CpGs) in *CD20* promoters almost 1000 bp upstream from the transcription start site to determine the mechanism of transcription up-regulation by 5-Aza treatment. Interestingly, CpG islands do not exist in the promoter site, and only 4 CG sequences can be observed in that region. Methylation of the 4 CG sites was not observed in the tumor cells from UPN 5 and RRBL1 cells using bisulfite sequencing (data not shown). Mechanisms other than DNA methylation of the *CD20* promoter may also be responsible for aberrant transcription down-regulation.

It is also possible that down-regulation of CD20 protein via such mechanisms as microRNA, protein folding, exportation, or glycosylation may occur. A recent report suggested the possibility that both *CD20* gene expression (at the pre- and posttranscriptional level) and protein down-regulation are related to the loss of CD20 protein expression after treatment with rituximab in vitro, resulting in rituximab resistance.[10] In addition, down-regulation of CD20 protein surface expression by internalization into the cytoplasm was also observed in some specific cases.[16,42] Further molecular analysis of the down-regulation of CD20 protein after treatment with rituximab is needed.

Another interesting finding in our study is that all of the patients showed a CD20-negative phenotypic change were diagnosed as DLBCL. Two cases were diagnosed as FL at their first admission, but both were transformed into DLBCL when a CD20-negative change was observed. Furthermore, a CD20-negative change was confirmed in all 5 cases using tumor cells derived from the bone marrow and/or cerebral fluid. These findings may suggest that the clinical entity and progression pattern is partly related to CD20-negative phenotypic transformation. Further studies will be needed to confirm this idea.

Genetic mutations in the *CD20* coding sequence were also observed in 2 cases, as shown in Table 2. These mutations led to amino acid alterations, including S97F and V247I, which are located at the second transmembrane domain and the C-terminal intracellular domain, respectively. A recent report suggested that neither site is recognized directly by rituximab.[43] Although it is possible that these alterations led to a conformational change in the CD20 protein that interferes with rituximab binding, a more attractive explanation may be that the loss of expression is much more critical for resistance to rituximab than we originally suspected. Preliminary data using fluorescence-labeled rituximab indicate that rituximab fails to bind to RRBL1 cells (CD20-negative B cells) in vitro (data not shown), and that ADCC and complement-dependent cytotoxicity (CDC) activity in vitro are significantly lower than in CD20-positive B cells (CDC; data not shown). These data suggest that the loss of antibody binding due to the down-regulation of antigen expression is one critical mechanism underlying rituximab resistance. Further investigation will be needed to expand these observations.

Our observations also revealed a population of cells that are rituximab-resistant despite the presence of CD20 protein expression as observed by FCM, IHC, and immunoblotting (data not shown). In those patients, molecular mechanisms other than a loss of protein expression may have occurred, such as an amino acid alteration resulting from a genetic mutation of the *MS4A1* gene, a posttranslational modification of the CD20 protein, abnormalities in the CD20 signal transduction pathway, antiapoptotic mechanisms of tumor cells, or aberrant metabolism of rituximab.[9,44,45] The detailed mechanisms of these and other possibilities are still unclear.

Finally, in the specific cases reported herein, 5-Aza can stimulate CD20 mRNA and protein expression, resulting in the restoration of rituximab sensitivity in vitro. The DNA methyltransferase inhibitors 5-azacytidine and 5-Aza have been used in patients suffering from hematologic malignancies such as myelodysplastic syndrome.[38,39,46] In the future, a combination of molecular targeting therapy using 5-Aza and rituximab may prove to be a unique strategy as a salvage therapy for CD20-negative transformed B-cell malignancies in certain patients. Further analysis of patients' primary cells and in vivo analysis using mouse xenograft lymphoma models are required.

Acknowledgments

We thank Tomoka Wakamatsu, Yukie Konishi, Mari Otsuka, Eriko Ushida, and Chieko Kataoka for valuable laboratory assistance. We also thank Yoko Kajiura, Yasuhiko Miyata, and Yuka Nomura for the FCM data analysis.

This work was supported in part by a Grant-in-Aid for Cancer Research (19-8) from the Ministry of Health, Labor and Welfare, a Grant-in-Aid from the National Institute of Biomedical Innovation, and

a Grant-in-Aid for Scientific Research (20591116) from the Ministry of Education, Culture, Sports, Science and Technology, Japan.

Authorship

J.H. and A.T. designed experiments, performed research, analyzed data, and wrote the paper; T.S. and K.S. prepared clinical samples and performed research; M.I. and S.N. performed pathologic analyses; H.K. and T.K. analyzed data, designed experiments, and interpreted data; and T.N. supervised experiments and wrote the paper.

Conflict-of-interest disclosure: H.K. is a consultant for a Kyowa Hakko Kogyo (Tokyo, Japan), and T.K. is funded by Chugai Pharmaceutical (Tokyo, Japan) and for Zenyaku Kogyo (Tokyo, Japan). The other authors declare no competing financial interests.

Correspondence: Akihiro Tomita, Department of Hematology and Oncology, Nagoya University Graduate School of Medicine, Tsurumai-cho 65, Showa-ku, Nagoya 466-8550, Japan; e-mail; atomita@med.nagoya-u.ac.jp.

References

1. Cheson BD. Monoclonal antibody therapy for B-cell malignancies. Semin Oncol. 2006;33:S2-14.
2. Imai K, Takaoka A. Comparing antibody and small-molecule therapies for cancer. Nat Rev Cancer. 2006;6:714-727.
3. Coiffier B, Lepage E, Briere J, et al. CHOP chemotherapy plus rituximab compared with CHOP alone in elderly patients with diffuse large-B-cell lymphoma. N Engl J Med. 2002;346:235-242.
4. Herold M, Haas A, Srock S, et al. Rituximab added to first-line mitoxantrone, chlorambucil, and prednisolone chemotherapy followed by interferon maintenance prolongs survival in patients with advanced follicular lymphoma: an East German Study Group Hematology and Oncology Study. J Clin Oncol. 2007;25:1986-1992.
5. Forstpointner R, Unterhalt M, Dreyling M, et al. Maintenance therapy with rituximab leads to a significant prolongation of response duration after salvage therapy with a combination of rituximab, fludarabine, cyclophosphamide, and mitoxantrone (R-FCM) in patients with recurring and refractory follicular and mantle cell lymphomas: results of a prospective randomized study of the German Low Grade Lymphoma Study Group (GLSG). Blood. 2006;108:4003-4008.
6. Habermann TM, Weller EA, Morrison VA, et al. Rituximab-CHOP versus CHOP alone or with maintenance rituximab in older patients with diffuse large B-cell lymphoma. J Clin Oncol. 2006;24:3121-3127.
7. Pfreundschuh M, Trumper L, Osterborg A, et al. CHOP-like chemotherapy plus rituximab versus CHOP-like chemotherapy alone in young patients with good-prognosis diffuse large-B-cell lymphoma: a randomised controlled trial by the MabThera International Trial (MInT) Group. Lancet Oncol. 2006;7:379-391.
8. Igarashi T, Kobayashi Y, Ogura M, et al. Factors affecting toxicity, response and progression-free survival in relapsed patients with indolent B-cell lymphoma and mantle cell lymphoma treated with rituximab: a Japanese phase II study. Ann Oncol. 2002;13:928-943.
9. Smith MR. Rituximab (monoclonal anti-CD20 antibody): mechanisms of action and resistance. Oncogene. 2003;22:7359-7368.
10. Czuczman MS, Olejniczak S, Gowda A, et al. Acquirement of rituximab resistance in lymphoma cell lines is associated with both global CD20 gene and protein down-regulation regulated at the pretranscriptional and posttranscriptional levels. Clin Cancer Res. 2008;14:1561-1570.
11. Olejniczak SH, Hernandez-Ilizaliturri FJ, Clements JL, Czuczman MS. Acquired resistance to rituximab is associated with chemotherapy resistance resulting from decreased Bax and Bak expression. Clin Cancer Res. 2008;14:1550-1560.
12. Macor P, Tripodo C, Zorzet S, et al. In vivo targeting of human neutralizing antibodies against CD55 and CD59 to lymphoma cells increases the antitumor activity of rituximab. Cancer Res. 2007; 67:10556-10563.
13. Cruz RI, Hernandez-Ilizaliturri FJ, Olejniczak S, et al. CD52 over-expression affects rituximab-associated complement-mediated cytotoxicity but not antibody-dependent cellular cytotoxicity: preclinical evidence that targeting CD52 with alemtuzumab may reverse acquired resistance to rituximab in non-Hodgkin lymphoma. Leuk Lymphoma. 2007;48:2424-2436.
14. Terui Y, Sakurai T, Mishima Y, et al. Blockade of bulky lymphoma-associated CD55 expression by RNA interference overcomes resistance to complement-dependent cytotoxicity with rituximab. Cancer Sci. 2006;97:72-79.
15. Takei K, Yamazaki T, Sawada U, Ishizuka H, Aizawa S. Analysis of changes in CD20, CD55, and CD59 expression on established rituximab-resistant B-lymphoma cell lines. Leuk Res. 2006; 30:625-631.
16. Jilani I, O'Brien S, Manshuri T, et al. Transient down-modulation of CD20 by rituximab in patients with chronic lymphocytic leukemia. Blood. 2003;102:3514-3520.
17. Bannerji R, Kitada S, Flinn IW, et al. Apoptotic-regulatory and complement-protecting protein expression in chronic lymphocytic leukemia: relationship to in vivo rituximab resistance. J Clin Oncol. 2003;21:1466-1471.
18. Treon SP, Mitsiades C, Mitsiades N, et al. Tumor cell expression of CD59 is associated with resistance to CD20 serotherapy in patients with B-cell malignancies. J Immunother. 2001;24:263-271.
19. Golay J, Lazzari M, Facchinetti V, et al. CD20 levels determine the in vitro susceptibility to rituximab and complement of B-cell chronic lymphocytic leukemia: further regulation by CD55 and CD59. Blood. 2001;98:3383-3389.
20. Kinoshita T, Nagai H, Murate T, Saito H. CD20-negative relapse in B-cell lymphoma after treatment with rituximab. J Clin Oncol. 1998;16:3916.
21. Schmitz K, Brugger W, Weiss B, Kaiserling E, Kanz L. Clonal selection of CD20-negative non-Hodgkin's lymphoma cells after treatment with anti-CD20 antibody rituximab. Br J Haematol. 1999;106:571-572.
22. Davis TA, Czerwinski DK, Levy R. Therapy of B-cell lymphoma with anti-CD20 antibodies can result in the loss of CD20 antigen expression. Clin Cancer Res. 1999;5:611-615.
23. Chu PG, Chen YY, Molina A, Arber DA, Weiss LM. Recurrent B-cell neoplasms after rituximab therapy: an immunophenotypic and genotypic study. Leuk Lymphoma. 2002;43:2335-2341.
24. Massengale WT, McBurney E, Gurtler J. CD20-negative relapse of cutaneous B-cell lymphoma after anti-CD20 monoclonal antibody therapy. J Am Acad Dermatol. 2002;46:441-443.
25. Kennedy GA, Tey SK, Cobcroft R, et al. Incidence and nature of CD20-negative relapses following rituximab therapy in aggressive B-cell non-Hodgkin's lymphoma: a retrospective review. Br J Haematol. 2002;119:412-416.
26. Alvaro-Naranjo T, Jaen-Martinez J, Guma-Padro J, Bosch-Princep R, Salvado-Usach MT. CD20-negative DLBCL transformation after rituximab treatment in follicular lymphoma: a new case report and review of the literature. Ann Hematol. 2003;82:585-588.
27. Clarke LE, Bayerl MG, Ehmann WC, Helm KF. Cutaneous B-cell lymphoma with loss of CD20 immunoreactivity after rituximab therapy. J Cutan Pathol. 2003;30:459-462.
28. Haidar JH, Shamseddine A, Salem Z, et al. Loss of CD20 expression in relapsed lymphomas after rituximab therapy. Eur J Haematol. 2003;70:330-332.
29. Rawal YB, Nuovo GJ, Frambach GE, Porcu P, Baiocchi RA, Magro CM. The absence of CD20 messenger RNA in recurrent cutaneous B-cell lymphoma following rituximab therapy. J Cutan Pathol. 2005;32:616-621.
30. Goteri G, Olivieri A, Ranaldi R, et al. Bone marrow histopathological and molecular changes of small B-cell lymphomas after rituximab therapy: comparison with clinical response and patients outcome. Int J Immunopathol Pharmacol. 2006; 19:421-431.
31. Ferreri AJ, Dognini GP, Verona C, Patriarca C, Doglioni C, Ponzoni M. Re-occurrence of the CD20 molecule expression subsequent to CD20-negative relapse in diffuse large B-cell lymphoma. Haematologica. 2007;92:e1-2.
32. Tomita A, Hiraga J, Kiyoi H, et al. Epigenetic regulation of CD20 protein expression in a novel B-cell lymphoma cell line, RRBL1, established from a patient treated repeatedly with rituximab-containing chemotherapy. Int J Hematol. 2007;86: 49-57.
33. Harris NL, Jaffe ES, Diebold J, et al. World Health Organization classification of neoplastic diseases of the hematopoietic and lymphoid tissues: report of the Clinical Advisory Committee meeting-Airlie House, Virginia, November 1997. J Clin Oncol. 1999;17:3835-3849.
34. Cheson BD, Horning SJ, Coiffier B, et al. Report of an international workshop to standardize response criteria for non-Hodgkin's lymphomas: NCI Sponsored International Working Group. J Clin Oncol. 1999;17:1244.
35. Ninomiya M, Abe A, Yokozawa T, et al. Establishment of a myeloid leukemia cell line, TRL-01, with MLL-ENL fusion gene. Cancer Genet Cytogenet. 2006;169:1-11.
36. Atsumi A, Tomita A, Kiyoi H, Naoe T. Histone deacetylase 3 (HDAC3) is recruited to target promoters by PML-RARalpha as a component of the N-CoR co-repressor complex to repress transcription in vivo. Biochem Biophys Res Commun. 2006;345:1471-1480.
37. Tomita A, Buchholz DR, Obata K, Shi YB. Fusion protein of retinoic acid receptor alpha with promyelocytic leukemia protein or promyelocytic leukemia zinc finger protein recruits N-CoR-TBLR1 corepressor complex to repress transcription in vivo. J Biol Chem. 2003;278: 30788-30795.
38. Egger G, Liang G, Aparicio A, Jones PA. Epigenetics in human disease and prospects for epigenetic therapy. Nature. 2004;429:457-463.
39. Yoo CB, Jones PA. Epigenetic therapy of cancer: past, present and future. Nat Rev Drug Discov. 2006;5:37-50.

40. van Oers MH, Klasa R, Marcus RE, et al. Rituximab maintenance improves clinical outcome of relapsed/resistant follicular non-Hodgkin's lymphoma, both in patients with and without rituximab during induction: results of a prospective randomized phase III intergroup trial. Blood. 2006;108:3295-3301.
41. Himmelmann A, Riva A, Wilson GL, Lucas BP, Thevenin C, Kehrl JH. PU.1/Pip and basic helix loop helix zipper transcription factors interact with binding sites in the CD20 promoter to help confer lineage- and stage-specific expression of CD20 in B lymphocytes. Blood. 1997;90:3984-3995.
42. Lapalombella R, Yu B, Triantafillou G, et al. Lenalidomide down-regulates the CD20 antigen and antagonizes direct and antibody-dependent cellular cytotoxicity of rituximab on primary chronic lymphocytic leukemia cells. Blood. 2008;113:5180-5185.
43. Binder M, Otto F, Mertelsmann R, Veelken H, Trepel M. The epitope recognized by rituximab. Blood. 2006;108:1975-1978.
44. Bonavida B. Rituximab-induced inhibition of antiapoptotic cell survival pathways: implications in chemo/immunoresistance, rituximab unresponsiveness, prognostic and novel therapeutic interventions. Oncogene. 2007;26:3629-3636.
45. Glennie MJ, French RR, Cragg MS, Taylor RP. Mechanisms of killing by anti-CD20 monoclonal antibodies. Mol Immunol. 2007;44:3823-3837.
46. Laird PW. Cancer epigenetics. Hum Mol Genet. 2005;14:R65-R76.

Int J Hematol (2009) 90:37–43
DOI 10.1007/s12185-009-0337-y

ORIGINAL ARTICLE

High-resolution melting analysis for a reliable and two-step scanning of mutations in the tyrosine kinase domain of the chimerical *bcr-abl* gene

Yuko Doi · Daisuke Sasaki · Chiharu Terada · Sayaka Mori · Kazuto Tsuruda · Emi Matsuo · Yasushi Miyazaki · Kazuhiro Nagai · Hiroo Hasegawa · Katsunori Yanagihara · Yasuaki Yamada · Shimeru Kamihira

Received: 12 March 2009 / Revised: 7 April 2009 / Accepted: 22 April 2009 / Published online: 23 May 2009

Abstract For relevant imatinib therapy against Philadelphia (Ph)-positive leukemias, it is essential to monitor mutations in the chimerical *bcr-abl* tyrosine kinase domain (TKD). However, there is no universally acceptable consensus on how to efficiently identify mutations in the target TKD. Recently, high-resolution melting (HRM) technology was developed, which allows gene scanning using an inexpensive generic heteroduplex-detecting dsDNA-binding dye. This study aimed to validate the introduction of HRM in a practical clinical setting for screening of mutations in sporadic sites of the chimerical *bcr-abl* TKD. All chimerical and wild-type *abl* TKD regions selectively amplified were used for HRM assays and direct sequencing. The HRM test had approximately 5–90% detection sensitivity for mutations. In contrast to mixture samples with mutant and wild-type cells, all mutant cell samples had indeterminate melting curves equivalent to those of the wild-type due to formation of only a homodulex. This issue was improved by the addition of exogenous wild-type DNA after PCR. Subsequently, HRM results gave a high accordance rate of 97.8% (44/45 samples) compared to the sequencing data. The discordant results in one appear to be due to unsuccessful amplification. Thus, HRM may be considered to be suitable for reliable scanning of mutations in the chimerical *abl* TKD in a clinical setting.

Keywords Ph · *bcr-abl* · Mutation · Melting analysis · HRM

Y. Doi · D. Sasaki · C. Terada · S. Mori · K. Tsuruda · K. Nagai · H. Hasegawa · K. Yanagihara · Y. Yamada · S. Kamihira (✉)
Department of Laboratory Medicine,
Nagasaki University Graduate School
of Biomedical Sciences, 1-7-1 Sakamoto,
Nagasaki 852-8501, Japan
e-mail: kamihira@nagasaki-u.ac.jp

E. Matsuo · Y. Miyazaki
Department of Hematology,
Nagasaki University Graduate School
of Biomedical Sciences, 1-7-1 Sakamoto,
Nagasaki 852-8501, Japan

1 Introduction

The chemical agent, imatinib, has a high therapeutic response for diseases carrying the chimerical *bcr-abl* gene. For example, the first imatinib treatment was reported to give approximately 80 and 60% complete molecular response rates in chronic myelogenous leukemia (CML) and Philadelphia (Ph)-positive acute lymphoblastic leukemia (ALL), respectively [1, 2]. However, in many cases, mutations in the chimerical *abl* tyrosine kinase domain (TKD) were revealed to precede resistance to imatinib, resulting in disease relapse and progression to advanced disease. At present, although it is known that there are several causative factors in resistance, such as expression of a rapid drug efflux protein and non-*bcr-abl*-dependent transformation involving the *src* family, TKD mutations in the chimerical gene are thought to play a major role in resistance acquisition [3]. Therefore, detection of mutations becomes essential in cases treated with imatinib. Moreover, mutations associated with imatinib therapy emerge as a Ph-positive subclone from minimal residual leukemia (MRD) even in the hematological remission period [4, 5]. This indicates the need for highly sensitive tests to detect only Ph-positive leukemic clones. To date, several methods to analyze mutations including direct and subcloning sequencing have been employed, but the respective methods have merits and demerits and are not

always sensitive [6]. Recently, to analyze genetic variations (SNPs, mutations and methylations), a novel melting analysis called high-resolution melting (HRM) with an automated instrument and real-time PCR apparatus was used [7, 8]. HRM is used to characterize samples according to their dissociation profile as they transit from double-strand DNA (dsDNA) to single-strand (ssDNA). Therefore, mixture samples with mutant and wild-type cells are easily identified by differences in melting curve shapes. Mutant sequence variants produce a Tm shift compared with the wild-type [9]. In addition, it is a reliable- and closed-tube system without high-cost fluorescence probes [10, 11]. Thus, to introduce HRM assays in clinical settings to detect Ph-positive subclones with *bcr-abl* kinase domain mutations, the relevance and validation of the assay prior to direct sequencing was studied.

2 Materials and methods

2.1 Samples and processing of cDNA

A total of 19 Ph-positive samples were used, consisting of 10 unlinked and already mutation-known specimens, 8 fresh practical samples from 6 patients with CML, 2 patients with ALL and one sample from a Ph-positive K562 cell line. All patients with Ph-positive leukemias were being treated with imatinib at 400–800 mg per day and had hematological remission, but were positive for *bcr-abl* real-time RT PCR. As controls, 16 peripheral blood samples from normal volunteers and 10 cell lines consisting of HTLV-1-associated cell lines (Hut102, KK1, KOB, OMT, MT2, SO4, ST1), T cell lines of Jurkat and MOLT4, and the monocytic line U937 were used.

Total RNA was extracted from total leukocyte guanidinium thiocyanate lysates using ISOGEN (Nippon gene, Toyama, Japan). cDNA was synthesized using oligo-dT primers and Superscript III reverse transcriptase (Invitrogen, Carsland, CA, USA). Practical and stocked samples used in this study were applied under the approval (15040708) of the ethics committee and the condition of the criteria of the Japanese Association of Laboratory Medicine.

2.2 Study design for HRM assay in the chimerical *abl* TKD region

Our study for the detection of mutation was designed in a two-step manner: firstly, genetic alteration screening by HRM analysis (Fig. 1), using the LightCycler 480 (Roche Molecular System, Alameda, CA, USA) for HRM and real-time thermal cycling; secondly, only samples positively screened by HRM were directly sequenced. First of all, each sample was examined for *bcr-abl* chimerical status by

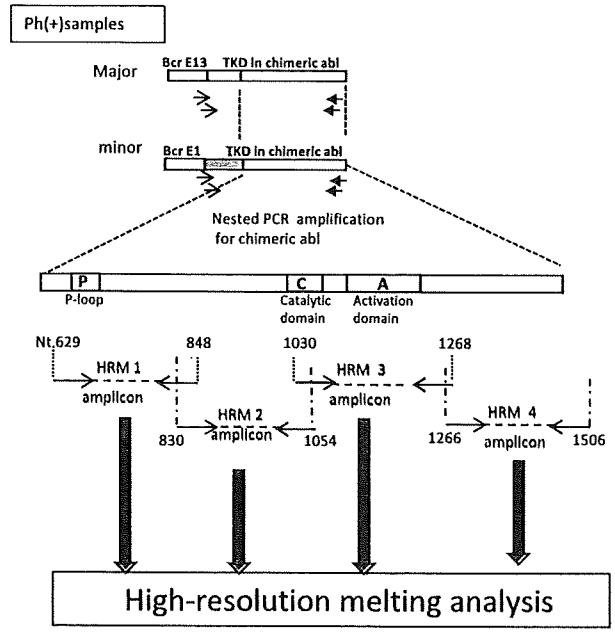

Fig. 1 Study design of high-resolution melting (HRM) and the structure of the tyrosine kinase domain (TKD). Firstly, a part of chimerical *bcr-abl* TKD is selectively amplified by nested PCR. Using amplified chimerical *bcr-abl* products as a template, the second PCR for the HRM assay is performed, generating four intercalating dye amplicons, HRM-1, -2, -3 and -4. Then, HRM analyses were done by using the LightCycler Gene Scanning Application

the conventional method [12]. If positive for major or minor chimerical types, these *bcr-abl* kinase domains were selectively amplified, generating a fragment of 1504 bp for b2/a2 and 1579 bp for b3/a2, using primers previously reported [13].

For HRM analysis, PCR products of 50–250 bp length are recommended for best discrimination. Therefore, we applied a modified method previously reported by Poláková et al. [10], generating 4 amplicons, designated as HRM1, 2, 3 and 4 of 220, 225, 239 and 241 bp, corresponding to nt 629–848, 830–1054, 1030–1268, and 1266–1506 (NM_005157), respectively. For HRM, a PCR reaction was performed in 20 µl reaction volumes containing 1 µl of 1/200 diluted template generated as described above, Master Mix, Taq DNA polymerase, dNTP mix, HRM dye, 3 mM $MgCl_2$, primers [10], and 1 M GC melt, according to the instructions of Roche Applied Science (Manheim, Germany). The PCR was monitored by real-time cycling and a strong fluorescent signal was generated only when bound to dsDNA, that is the touchdown PCR cycling and HRM conditions [14]. HRM melting curve data were obtained by slowly increasing the temperature, from 60 to 90°C at a rate of 100 acquisitions per 1°C. The melting status and changes in Tm value were analyzed using the Roche HRM algorithm (Gene Scanning Software, Roche Supplied Science, Manheim, Germany),

depicting graphs of fluorescence-normalized and temperature-shifted melting curves and difference plots. The cell line K562 was used as a wild-type reference sample.

2.3 Sequencing

In this study, to compare to accuracy of HRM analysis, regardless of the first-step negative samples, all of the samples used were confirmed by sequencing the regions of the selectively amplified chimerical *abl* TKD, as well as *abl* TKD from Ph-negative controls using a Big Dye terminator kit Ver 3.1 (Applied Biosystems, Carsland, CA, USA) and the ABl Prism 3130 Genetic Analyzer (Applied Biosystems) according to the manufacturer's instructions.

3 Results

3.1 HRM assay validation

For HRM scoring, Ph(+) K562 was set up as a wild-type genotype and the 2 or 3 normal blood samples were monitored as negative controls. First of all, using three different samples with mutations, HRM analysis in duplicate was performed, generating constant positive melting curves both in terms of shape and peak height with a range of melting temperatures (Tm) from 84 to 86°C (Fig. 2). On the other hand, 16 samples without the Ph-chromosome constantly produced the wild-type scanning profiles according to the Roche HRM program, as shown in Fig. 3 (normalized and temperature-shifted melting curves and difference plots).

Interestingly, as shown in Fig. 2b, no correlation was observed between fluorescence heights and the ratio of the mutant and wild-type: the peak was higher in mixture samples with mutant and wild-type cells than samples with only mutant clones. To address this strange relation, variable mixture samples with mutant and wild-type cells diluted by exogenous control DNA from wild-type cells were subjected to HRM assay. Figure 4 shows that samples containing only mutant cells (bottom graph) produced indeterminate signals with low peaks, but the mixture samples containing variable wild-type cell burden (5–90%) displayed apparently higher peaks, indicating the existence of mutation. This shows that 100% mutant samples may become false negative, indistinguishable from only wild-type patterns. To form only homoduplex, dsDNA in either mutant or wild-type DNA probably accounted for the indeterminate evaluation in all mutant or wild-type samples.

Accordingly, to avoid false negatives in samples with all mutant cells, we organized screen mutations using two divided samples; one was an original and the other mixed with exogenous wild-type cells, as shown in Fig. 5. Using this strategy, the test performance of HRM was examined in this study.

3.2 HRM assay results

The HRM assay was blindly examined in duplicate by a single researcher and then compared to sequence data. As summarized in Table 1, the HRM test was positive for 13 (68.4%) of 19 Ph-positive leukemias, including a Ph-positive K562 cell line. Using the same amplicons as

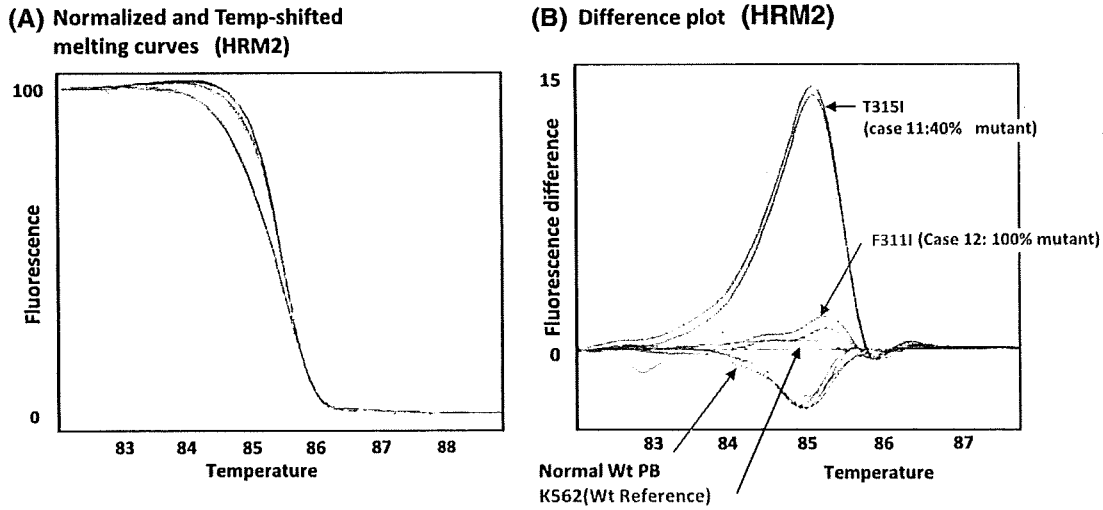

Fig. 2 Validation of the HRM assay using samples with 100% mutant cells and samples with variable % mutant cells. Duplicate assays gave rise to the similar results, indicating the good reproducibility in both normalized and temperature-shifted melting curves and difference plots. Ph-positive K562 cells were used as a wild-type (Wt) reference

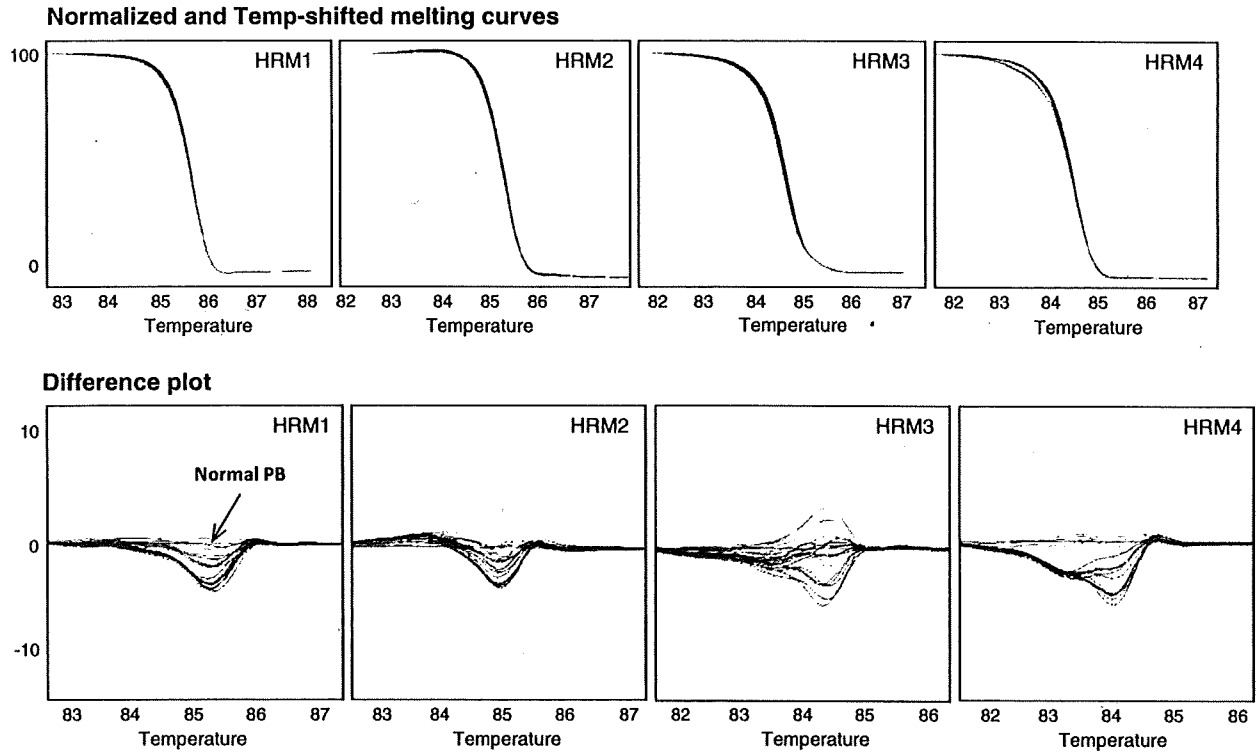

Fig. 3 Validation of HRM test performance using negative controls with wild-type TKD demonstrated by direct sequencing in peripheral blood from 16 healthy persons and 9 hematopoietic cell lines, excluding the U937 cell line. All 4 HRM analyses were evaluated to be wild-type by both normalized-temperature-shifted melting curves according to the Gene Scanning Application Algorithm. Normal peripheral blood from volunteers was used as a wild-type reference

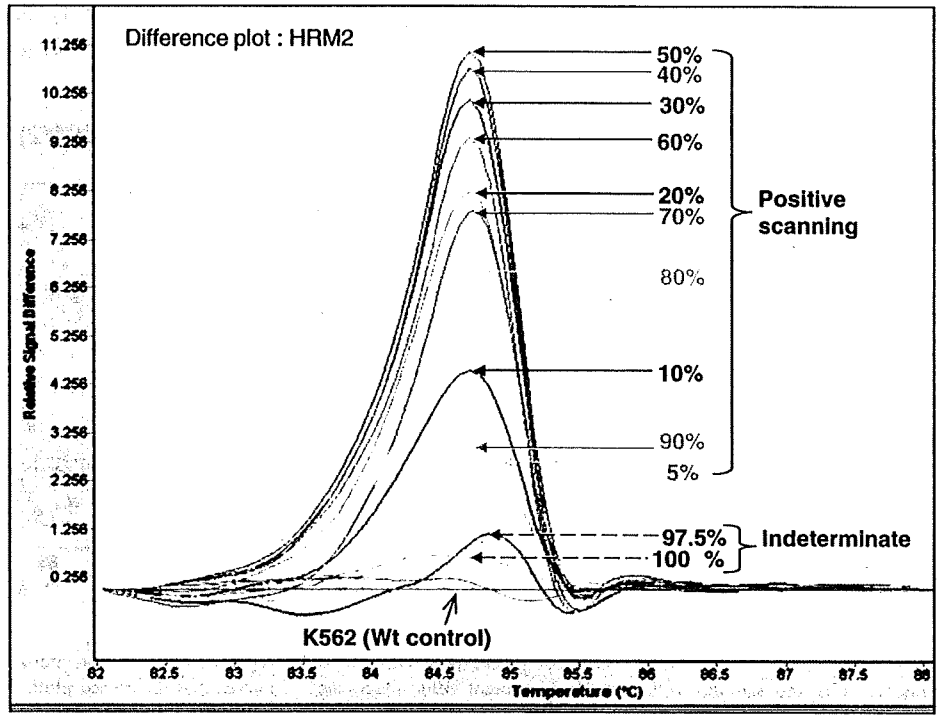

Fig. 4 Changes in the heights of peaks and Tm values depending on the difference in the mixture ratio of mutant and wild-type cells. HRM assay revealed indeterminate signals in samples with only mutant cells (around 100% mutant cell samples). On the other hand, the mixture samples diluted to 5% mutant cells produced typical positive scanning patterns, indicating that the best mixture ratio was 50 versus 50%

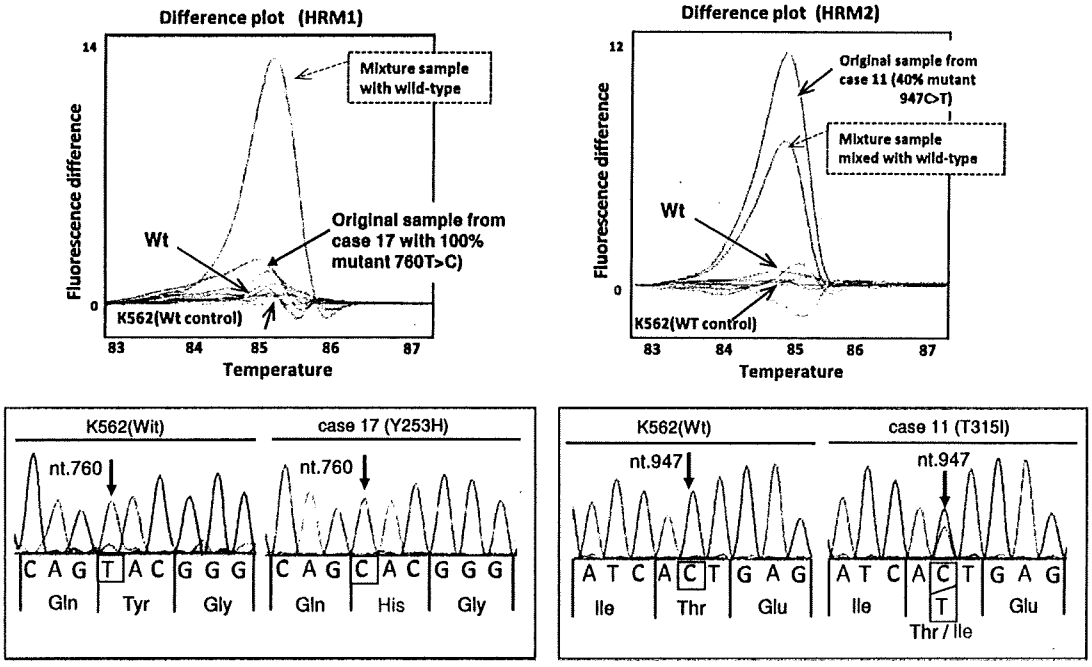

Fig. 5 Representative cases (A and B) of HRM and sequencing analyses. The left panel showed that the addition of wild-type DNA into the 100% mutant (760 T > C) sample made discrimination easy. On the other hand, the right panel showed that the change in the melting curves between the original (947 C > T) and the mix allowed discrimination

above, direct sequencing identified 14 missense mutations (73.6%) out of 19 Ph(+) leukemias. The positive and negative accordance rate of both tests was 94.7% among 19 Ph(+ or −) samples. The discrepancy in sample no. 5, negative in the HRM and positive in the sequencing, was expected before HRM analysis, because the PCR efficiency was not so good. As expected, the direct sequencing disclosed a problematic issue for PCR, in that a mutation (nt 838) existed within the annealing sequence (nt830-849) of the primer.

Next, of 26 Ph-negative samples consisting of 10 cell lines and 16 normal blood controls, HRM assays produced negative findings in all but one. The positive one for HRM was U937 derived from myelomonocytoid leukemic cells. The sequencing revealed a mutation of E308V, which was expected to be somatic as it is one of the oncogenes.

Conclusively, the accordance rate of the two methods was 97.8% in all 45 cases of Ph-positive/-negative leukemias and controls.

4 Discussion

Most patients with Ph-positive leukemias, especially chronic CML, who receive imatinib as first-line therapy achieve good cytogenetic and molecular responses. However, long-term molecular studies suggest that around 25–30% of patients seem not to achieve successful responses and undergo disease progression. Major causes of imatinib resistance include the emergence of leukemic clones with mutations in the tyrosine kinase domain of *bcr-abl*. This indicates that it is necessary to screen for mutations in early phase of the emergence of mutation clones. Unfortunately, there is generally no acceptable consensus on when and by which technology the TKD mutations should be screened. At present, direct sequencing, denaturing high-performance liquid chromatography (D-HPLC), denaturing gradient gel electrophoresis (DGGE), allele-specific oligonucleotide-polymerase chain reaction (ASO-PCR) and pyro-sequencing are available, but the respective methods have merits and demerits for practical clinical settings [6]. A novel technology of HRM with the development of instruments and saturating intercalating dyes is emerging for the detection of nucleic acid sequence variations and is now applied in practical diagnostic settings [7, 15]. The two-step method allows to avoid the direct sequencing for the entire region of all samples.

In this study, the HRM in our system was shown to efficiently and simply differentiate mutations in the chimerical *bcr-abl* TKD region by using LightCycler technology and a software algorithm. In particular, it is noteworthy that mixture samples with mutant and wild-type cells were easily detectable with high sensitivity (approximately 5%). On the other hand, samples with all

Table 1 Summary of the results on mutations examined by both HRM and direct sequencing analyses

Sample	Clinical dx	bcr-abl	HRM results	TKD	nt substitute	Exon
Unlinked						
1	CML	Major	Mut	Y253F	761 A > T	4
2	CML	Major	Mut	Y253H	760 T > C	4
3	CML	Major	Mut	E255 V	767 A > T	4
4	CML	Major	Mut	E255 K	766 G > A	4
5	CML	Major	NE	E279 K	838 G > A	5
6	CML	Major	Mut	T315I	947 C > T	6
7	CML	Major	Mut	F317L	954 C > A	6
8	CML	Major	Mut	M351T	1055 T > C	6
9	CML	Major	Mut	H396R	1190 A > G	7
10	CML	Major	Mut	F486S	1460 T > C	9
Fresh						
11	CML	Major	Mut	T315I	947 C > T	6
12	CML	Major	Mut	F311I	934 T > A	6
13	CML	Major	Mut	L370R	1112 T > G	7
14	CML	Major	Wt	Wt		
15	CML	Major	Wt	Wt		
16	CML	Major	Wt	Wt		
17	ALL	Minor	Mut	Y253H	760 T > C	4
18	ALL	Minor	Wt	Wt		
Cell lines						
19	K562	Major	Wt	Wt		
20	U937	(–)	Mut	E308V	926 A > T	5
21	KOB	(–)	Wt	Wt		
22	KK1	(–)	Wt	Wt		
23	ST1	(–)	Wt	Wt		
24	SO4	(–)	Wt	Wt		
25	OMT	(–)	Wt	Wt		
26	MT2	(–)	Wt	Wt		
27	Hut102	(–)	Wt	Wt		
28	Jurkat	(–)	Wt	Wt		
29	MOLT4	(–)	Wt	Wt		
Normal PB						
30–45		(–)	Wt	Wt		

Mut mutation, *Wt* wild-type, *NE* not evaluated

mutant cells often present with indeterminate low peaks in difference plots, causing confusing interpretations. This is probably the main defect in this HRM technology, resulting from a dependency on heteroduplex formation due to the mixture ratio of the mutant and wild-type. Therefore, to avoid false negatives with samples containing all mutant cells, it was shown that the addition of exogenous control DNA was useful (Figs. 4, 5). Actually, since the ratio of mutant cells in the samples is unknown in practical samples, we adopted an HRM assay system, which measures using a double feature: an original one and mixtures of the mutant and exogenous wild-type DNA in the ratio of 1:1. Practical examples are shown in Fig. 5, indicating that the mixed sample (left panel) makes it easy to discriminate, whereas the change in the positive peak pattern was tolerable if a 40% mutant sample was diluted to 50%.

Finally, our HRM results were in agreement in all but one of 45 samples with an accordance rate of 97.8% compared with sequencing data. The discrepancy in the results in one sample was expected due to an accidental relation between the primer and mutation sites, as described above. The quality of HRM is thought to be highly dependent on real-time amplification, so that we are now revising part of the primer set and appropriate sequence length for HRM.

Clearly, this is a rapid, simple, accurate screening method using HRM technology for chimerical *bcr-abl* TKD mutations involved in resistance to imatinib. Since resistant Ph-subclones emerge from MRD and increase step by step in parallel with the long imatinib therapy duration, the HRM assay system is a suitable and useful method to better manage Ph-positive leukemias, for example, to decide on dose escalation or cessation of imatinib, alternation of new drugs or different therapies with dasatinib and bone marrow transplantation. Actually, we are applying this method in a routine clinical setting prior to sequencing to select only mutation-positive samples.

References

1. O'Brien SG, Guilhot F, Larson RA, Gathmann I, Baccarani M, Cervantes F, et al. Imatinib compared with interferon and low-dose cytarabine for newly diagnosed chronic-phase chronic myeloid leukemia. N Engl J Med. 2003;348:994–1004. doi: 10.1056/NEJMoa022457.
2. Matsuo E, Miyazaki Y, Tsutsumi C, Inoue Y, Yamasaki R, Hata T, et al. Imatinib provides durable molecular and cytogenetic responses in a practical setting for both newly diagnosed and previously treated chronic myelogenous leukemia: a study in Nagasaki Prefecture, Japan. Int J Hematol. 2007;85:132–9. doi: 10.1532/IJH97.06157.
3. Hughes T. ABL kinase inhibitor therapy for CML: baseline assessments and response monitoring. Hematology. 2006;211–8. American Society of Hematology.
4. Hughes T, Deininger M, Hochhaus A, Branford S, Radich J, Kaeda J, et al. Monitoring CML patients responding to treatment with tyrosine kinase inhibitors: review and recommendations for harmonizing current methodology for detecting BCR-ABL transcripts and kinase domain mutations and for expressing results. Blood. 2006;108:28–37. doi:10.1182/blood-2006-01-0092.
5. Branford S, Rudzki Z, Walsh S, Grigg A, Arthur C, Taylor K, et al. High frequency of point mutations clustered within the adenosine triphosphate-binding region of BCR/ABL in patients with chronic myeloid leukemia or Ph-positive acute lymphoblastic leukemia who develop imatinib (STI571) resistance. Blood. 2002;99:3472–5. doi:10.1182/blood.V99.9.3472.
6. Willis SG, Lange T, Demehri S, Otto S, Crossman L, Niederwieser D, et al. High-sensitivity detection of BCR-ABL kinase domain mutations in imatinib-naive patients: correlation with

clonal cytogenetic evolution but not response to therapy. Blood. 2005;106:2128–37. doi:10.1182/blood-2005-03-1036.
7. Wittwer CT, Reed GH, Gundry CN, Vandersteen JG, Prvor RJ. High-resolution genotyping by amplicon melting analysis using LCGreen. Clin Chem. 2003;9:853–60. doi:10.1373/49.6.853.
8. Zhou L, Wang L, Palais R, Pryor R, Wittwer CT. High-resolution DNA melting analysis for simultaneous mutation scanning and genotyping in solution. Clin Chem. 2005;51:1770–7. doi: 10.1373/clinchem.2005.054924.
9. Herrmann MG, Durtschi JD, Bromley LK, Wittwer CT, Voelkerding KV. Amplicon DNA melting analysis for mutation scanning and genotyping: cross-platform comparison of instruments and dyes. Clin Chem. 2006;52:494–503. doi:10.1373/clinchem.2005.063438.
10. Poláková KM, Lopotová T, Klamová H, Moravcová J. High-resolution melt curve analysis: initial screening for mutations in BCR-ABL kinase domain. Leuk Res. 2008;32:1236–43. doi: 10.1016/j.leukres.2008.01.010.
11. Grievink H, Stowell KM. Identification of ryanodine receptor 1 single-nucleotide polymorphisms by high-resolution melting using the LightCycler 480 System. Anal Biochem. 2008;374: 396–404. doi:10.1016/j.ab.2007.11.019.
12. Yanada M, Takeuchi J, Sugiura I, Akiyama H, Usui N, Yagasaki F, et al. High complete remission rate and promising outcome by combination of imatinib and chemotherapy for newly diagnosed BCR/ABL-positive acute lymphoblastic leukemia: a phase II study by the Japan Adult Leukemia Study Group. J Clin Oncol. 2006;2006(24):460–6. doi:10.1200/JCO.2005.03.2177.
13. Rulcová J, Zmeková V, Zemanová Z, Klamová H, Moravcová J. The effect of total-ABL, GUS and B2M control genes on BCR-ABL monitoring by real-time RT-PCR. Leuk Res. 2007;31:483–91. doi:10.1016/j.leukres.2006.07.021.
14. Krypuy M, Ahmed AA, Etemadmoghadam D, Hyland SJ; Australian Ovarian Cancer Study Group, DeFazio A, Fox SB, Brenton JD, Bowtell DD, Dobrovic A. High-resolution melting for mutation scanning of TP53 exons 5-8. BMC Cancer. 2007;7:168. doi:10,1186/1471-2407-7-168.
15. De Leeneer K, Coene I, Poppe B, De Paepe A, Claes K. Rapid and sensitive detection of BRCA1/2 mutations in a diagnostic setting: comparison of two high-resolution melting platforms. Clin Chem. 2008;54:982–9. doi:10.1373/clinchem.2007.098764.

Int J Hematol (2009) 89:319–325
DOI 10.1007/s12185-009-0263-z

ORIGINAL ARTICLE

Long-term efficacy of imatinib in a practical setting is correlated with imatinib trough concentration that is influenced by body size: a report by the Nagasaki CML Study Group

Mari Sakai · Yasushi Miyazaki · Emi Matsuo · Yukiyoshi Moriuchi · Tomoko Hata · Takuya Fukushima · Yoshitaka Imaizumi · Daisuke Imanishi · Jun Taguchi · Masako Iwanaga · Hideki Tsushima · Yoriko Inoue · Yumi Takasaki · Takeshi Tsuchiya · Minori Komoda · Koji Ando · Kensuke Horio · Yuji Moriwaki · Shinya Tominaga · Hidehiro Itonaga · Kazuhiro Nagai · Kunihiro Tsukasaki · Chizuko Tsutsumi · Yasushi Sawayama · Reishi Yamasaki · Daisuke Ogawa · Yasuhisa Kawaguchi · Shuichi Ikeda · Shinichiro Yoshida · Yasuyuki Onimaru · Masayuki Tawara · Sunao Atogami · Satoshi Koida · Tatsuro Joh · Masaomi Yamamura · Yuji Matsuo · Hisashi Soda · Hiroaki Nonaka · Itsuro Jinnai · Kazutaka Kuriyama · Masao Tomonaga

Received: 26 August 2008 / Revised: 9 January 2009 / Accepted: 27 January 2009 / Published online: 6 March 2009

Abstract Imatinib has dramatically improved long-term survival of chronic myelogenous leukemia (CML) patients. To analyze its efficacy in a practical setting, we registered most of CML patients in Nagasaki Prefecture of Japan. Of these, 73 patients received imatinib as an initial therapy. The overall survival rate of these patients was 88.7% at 6 years, and the cumulative complete cytogenetic response rate was 82.5% at 18 months. These results are comparable with the data of other reports including the IRIS study; however, the administered imatinib dose was smaller in our study than that in other reports. To address these discrepancies, we measured the trough concentration of imatinib among 35 patients. Although 39% of the patients were administered less than 400 mg/day, the trough level was comparable to those of previous reports. The trough level of imatinib showed a significant relationship with its efficacy, and was clearly related to dose of imatinib administrated and dose of imatinib divided by body surface area (BSA). Considering the smaller BSA of Japanese patients as compared to those of foreign origin, the results suggest that a lower dose of imatinib could maintain enough trough level and provided excellent results for the treatment of CML in our registry.

Keywords CML · Imatinib · Trough concentration

The affiliation details of the members of Nagasaki CML Study Group are given in Appendix.

M. Sakai · Y. Miyazaki (✉) · E. Matsuo · T. Hata · T. Fukushima · Y. Imaizumi · D. Imanishi · J. Taguchi · M. Iwanaga · T. Tsuchiya · M. Komoda · K. Ando · K. Horio · S. Tominaga · H. Itonaga · K. Nagai · K. Tsukasaki · M. Tomonaga
Department of Hematology and Molecular Medicine Unit, Atomic Bomb Disease Institute, Nagasaki University Graduate School of Biomedical Sciences, 1-12-4 Sakamoto, Nagasaki 852-8523, Japan
e-mail: y-miyaza@nagasaki-u.ac.jp

Y. Moriuchi · H. Tsushima · Y. Inoue · Y. Takasaki · Y. Moriwaki · C. Tsutsumi · Y. Sawayama · R. Yamasaki · D. Ogawa · Y. Kawaguchi · S. Ikeda · S. Yoshida · Y. Onimaru · M. Tawara · S. Atogami · S. Koida · T. Joh · M. Yamamura · Y. Matsuo · H. Soda · H. Nonaka · I. Jinnai · K. Kuriyama
Nagasaki CML Study Group, Nagasaki, Japan

1 Introduction

Imatinib, an inhibitor of the BCR-ABL fusion protein, has dramatically changed the treatment of chronic myelogenous leukemia (CML) [1–3]. The International Randomized Interferon versus STI571 (IRIS) phase III clinical trial revealed that imatinib provided better long-term survival compared to interferon (IFN) plus cytosine arabinoside (AraC) for patients with CML in chronic phase [4–6]. Imatinib produces a complete cytogenetic response (CCR) by reducing the number of CML cells and enables the recovery of hematopoiesis without Philadelphia chromosome (Ph). Imatinib further reduces the volume of CML clone to the levels only detectable by molecular techniques [5]. Based on the results of several clinical trials including

the IRIS study, imatinib administration (400 mg/day) has become the standard treatment for CML patients in chronic phase. We previously conducted an analysis of registered CML patients in Nagasaki prefecture of Japan capturing more than 80% of patients in this prefecture (approximate population of 1.44 million) to determine imatinib efficacy in a practical setting rather than in a clinical trial situation [7]. Reflecting the practical situation of daily clinic, clinical features of patients in our registration were different from those reported in the IRIS study in some aspects: older age, advanced Sokal score at diagnosis, and lower daily dose of imatinib administered in the Nagasaki Study. However, interestingly the survival and cytogenetic/molecular responses of these patients were comparable to those of the IRIS study.

In 2008, after more than 6 years of imatinib use, we performed a survival analysis of our CML patients to identify the long-term effect of imatinib therapy in a practical setting. During this analysis, we again noticed a good survival in our series similar to the IRIS study despite lower dose of imatinib administered in the Nagasaki Study. Recently, some reports on plasma trough concentration of imatinib were published [8, 9]. In one report, the trough imatinib plasma levels were associated with both cytogenetic and molecular responses, demonstrating the importance of imatinib concentration above 1002 ng/ml for good responses [8]. In another report, which was a part of the IRIS study, the plasma imatinib level differed widely among patients administered with 400 mg/day, and showed a significant but not clinically meaningful relationship of imatinib concentration with body weight and body surface area (BSA) of the patients [9]. In the same study, there was a significant correlation between the imatinib trough level (day 29 of treatment) and the long-term response as judged by cytogenetic or molecular analysis [9]. With these reported data, we hypothesized that the plasma concentration of imatinib rather than the administered dose might explain the clinical results of imatinib in our registration that would represent the practical daily clinic for CML patients.

To address this issue, we measured the trough concentration of plasma imatinib in patients administered with different doses of imatinib, and tested the relationship between its concentration and efficacy. We found that the imatinib trough concentration was comparable or higher in our analysis compared to those reported in the IRIS study and the French group studies, and it was significantly related to the clinical efficacy in a practical setting. These results suggested that the imatinib trough level would be a useful marker to determine the dose of imatinib administered in each patient balancing its efficacy and adverse effects.

2 Patients and methods

2.1 Patients

One hundred and thirty CML patients from 11 major hospitals were registered for the Nagasaki CML Study Group, Nagasaki Prefecture, Japan. As shown in our previous report, the registration included approximately 85% of the patients in the Nagasaki-Prefecture Tumor Registry [7]. The 130 patients included 74 newly diagnosed patients from December 2001 to March 2008 and 56 patients who were alive in December 2001, at the beginning of the registration when imatinib became widely available in Japan. Informed consent was obtained from 36 of the 130 patients to measure the trough concentration of imatinib, and it was measured in 35 patients (one sample was not suitable for the analysis). This study was approved by the Ethical Committees of the participating hospitals.

2.2 Measurement of plasma imatinib concentration

Peripheral blood was obtained from 36 patients within 24 ±2 h from the last imatinib administration. The plasma was immediately separated at 4°C by centrifugation and kept at −20°C until measurement. One sample was found not suitable for the analysis, so finally, 35 samples were analyzed. The plasma imatinib concentration of the 35 patients was measured at the Toray Research Center, Inc. (Nihonbashi, Tokyo, Japan) using liquid chromatography–tandem mass spectrometry method [10].

2.3 Clinical parameters including the response to the therapy

Overall survival (OS) was calculated from the day of diagnosis to the date of death (regardless of the cause of death), or the last follow-up date. The daily dose of imatinib was calculated as an average dose: total amount of imatinib taken was divided by the number of days of the certain period. Complete cytogenetic response (CCR) was defined as no Ph-positive metaphases in the sample. Real time reverse transcriptase-mediated quantitative polymerase chain reaction (RQ-PCR) was performed to identify the molecular response. In some cases, fluorescent in situ hybridization (FISH) analysis for bcr-abl fusion gene of peripheral blood neutrophils was also performed. In the cases only RQ-PCR or FISH results for bcr-abl fusion were available, CCR equivalent responses (bcr-abl/abl level <0.01 by RQ-PCR or below the detection limit of bcr-abl signal by FISH) were included in CCR. A threefold log reduction in the *bcr-abl* transcripts by RQ-PCR was determined to be a major molecular response (MMR). The

overall response to imatinib was evaluated using the criteria proposed by European LeukemiaNet [11].

2.4 Statistical analysis

Categorical parameters of the clinical characteristics were compared using the Chi-square or Fisher exact test, and the continuous parameters were compared using two-sample *t* test or the Wilcoxon rank-sum test. The imatinib dose between the two groups was treated as continuous or categorical data. The probabilities of CCR and OS were estimated by the Kaplan–Meier method. Linear regression was used to correlate baseline plasma trough concentration of imatinib with body weight, BSA, and imatinib dose divided by BSA. All statistical analyses were performed using JMP (SAS Institute, Inc., Cary, NC). A P values of <0.05 was considered statistically significant. All analyses were completed by April 30 2008.

3 Results

3.1 Characteristics of patients and long-term efficacy of imatinib as an initial treatment

The registration of CML patients started in December 2001. By March 2008, 130 patients were enrolled in this study including 99 patients who were registered before and 31 patients who were registered after July 2005 (Table 1).

Table 1 Clinical features of the patients

	All	Initial treatment	
		Imatinib	Others
Number of patients	130	73	57
Male/female	71/59	40/33	31/26
Age at diagnosis (median)	15–84 (56)	17–84 (57)	15–80 (55)
Clinical phase at diagnosis			
CP	105	61	44
AP	22	10	12
BC	2	2	0
Unknown	1	0	1
Time after diagnosis, years (median)	0.2–25.2 (5.5)	0.2–7 (3.2)	1.7–25.2 (9.6)
Sokal score at diagnosis			
Low	47	23	24
Intermediate	44	29	15
High	30	19	11
Unknown	9	2	7

CP Chronic phase, *AP* accelerated phase, *BC* blastic crisis

Imatinib was the first treatment for 73 patients, and 96% (70 out of 73 patients) including the 31 patients registered after July 2005, were still undergoing the imatinib treatment. Of the 130 patients 17 were died between 2001 and 2008 (12 patients by disease progression, 3 due to other malignancies, 1 by cerebral hemorrhage, and 1 by rhabdomyolysis).

The median daily dose of imatinib administered was 400 mg (range 0–600 mg) among 70 patients who were initially treated with and continued taking imatinib; 33% (23 of 70 patients) received less than 400 mg/day. To compare the long-term imatinib response between the IRIS study and the Nagasaki registry, a practical setting, we analyzed survival and cytogenetic response among 73 patients who received imatinib without prior treatment. The overall survival rate was 88.7% (95% CI = 79.3–98.1) at 5 years (Fig. 1a), and the accumulated rate of complete cytogenetic response was 82.5% (95% CI = 70.7–94.3) after 18 months of treatment (Fig. 1c). Data for cases in chronic and accelerated phase were also calculated separately (Fig. 1b, d).

The ELN has categorized the imatinib response as optimal, suboptimal, and failure based on the chronological monitoring of hematological, cytogenetic and molecular responses. We applied this response criterion to 70 patients (including those with other than chronic phase CML at diagnosis) who were initially treated with and also currently being treated with imatinib. Cytogenetic and molecular data were available for 51 out of 70 patients (death, 6 patients; lost follow-up, 4; insufficient data, 9). Imatinib response was judged as failure in 9 of these 51 patients, suboptimal in 6, and optimal in 36. Four of the 9 patients in the failure-response category had received imatinib 300 mg/day or less, but 8 out of 36 in the optimal response category had received less than 400 mg/day.

3.2 Trough concentration of imatinib and treatment response

Since the overall survival and cytogenetic response rate to imatinib was comparable to those observed in the IRIS study despite low dose of imatinib, we measured the plasma trough concentration of imatinib in 35 patients including 11 patients who had received IFN or other medication before imatinib was introduced (Table 1). Two patients were excluded from the analysis because of the additional IFN treatment and impaired renal function. The clinical features of the remaining 33 patients are listed in Table 2. Although 6 patients were in the accelerated phase at the time of diagnosis, all were in a chronic phase under imatinib for at least 6 months when the samples were obtained. The median dose of imatinib was 400 mg (range 100–600 mg), and 13 patients (39%) were treated with

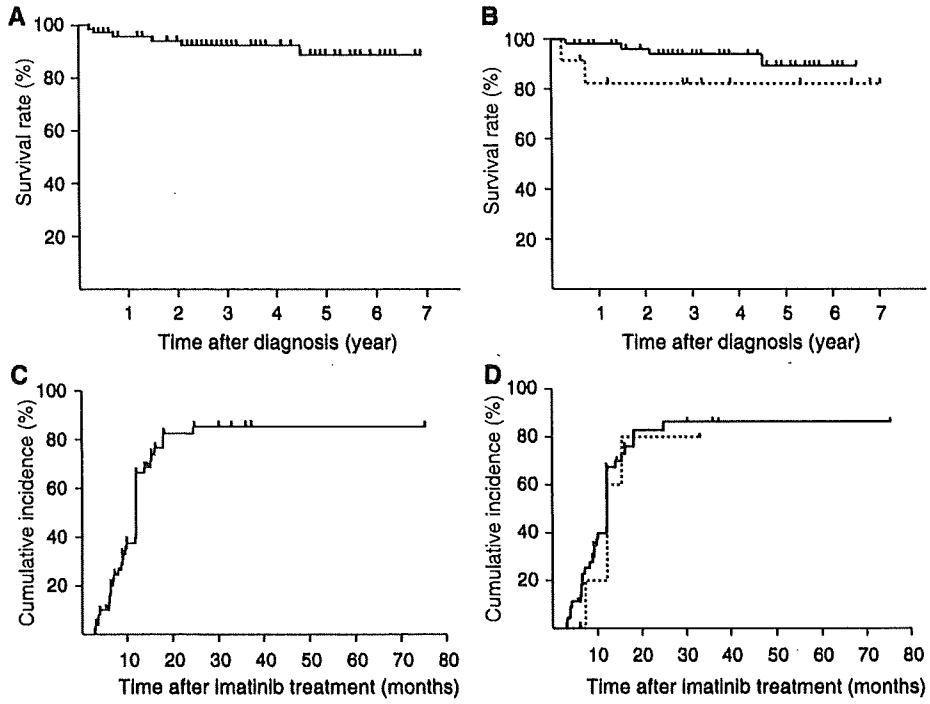

Fig. 1 Overall survival and cumulative cytogenetic response of patients whose initial treatment was imatinib. **a** Overall survival at 5 years was 88.7% in all cases ($n = 73$, 95% CI 79.3–98.1%), and **(b)** that of in chronic (*solid line*) and accelerated (*dotted line*) phases was 89.9 and 82.5%, respectively. **c** Cumulative cytogenetic response at 18 months was 82.5% in all cases ($n = 51$, 95% CI 70.7–94.3%), and **(d)** that of chronic (*solid line*) and accelerated (*dotted line*) phases was 82.9 and 80.0%, respectively

Table 2 Characteristics of patients whose imatinib concentration was measured

Male/female (number)	22/11
Initial imatinib treatment (yes/no)	22/11
Age at diagnosis, years (median)	17–82 (50)
Clinical phase at diagnosis	
CP	27
AP	6
BC	0
Time after diagnosis, years (median)	1.6–25.2 (4.9)
Duration of imatinib, years (median)	0.5–7.4 (4.2)
Dose of imatinib (mg/day)	
<200	3
200	1
300	9
400	19
600	1

CP Chronic phase, *AP* accelerated phase, *BC* blastic crisis

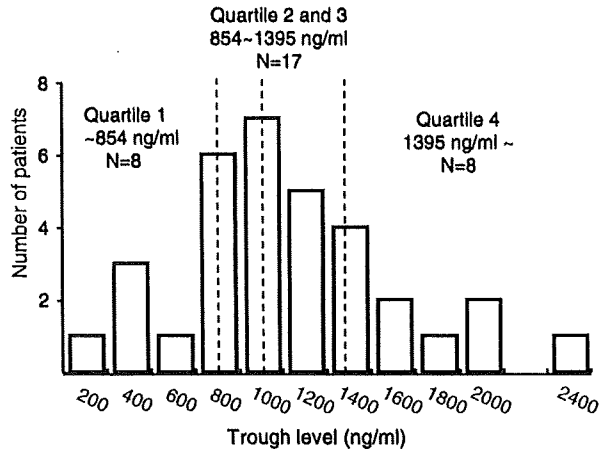

Fig. 2 Distribution of imatinib trough levels ($n = 33$). The *vertical dashed lines* represent the 25th, median, and 75th percentiles within quartiles 2 and 3

300 mg/day or less. As shown in Fig. 2, the median concentration was 1040 ng/ml (range 233–2420 ng/ml). We divided the patients into quartile groups (Q1–Q4) based on their imatinib trough level. The average of trough level of the lowest quartile (Q1) was 845 ng/ml, and that of upper quartile (Q4) was 1395 ng/ml. Trough concentration did not exhibit correlation with body weight of patients ($r^2 = 0.004$), or BSA ($r^2 < 0.001$), but it demonstrated significant correlation with the imatinib dose divided by BSA (dose/BSA, $r^2 = 0.28$, Fig. 3a–c) or by BW (dose/BW, $r^2 = 0.23$). However, even among those taking the same dose of 400 mg/day, the imatinib concentration was widely distributed (582–2420 ng/ml). Interestingly, the influence of body size on the plasma concentration of imatinib seemed stronger among those taking lower dose of imatinib: r^2 value in the concentration and dose/BSA among those with 200 mg was 0.65 ($P = 0.1922$) and those with 300 mg or more was 0.008 and 0.018 ($P = 0.8158$ and 0.5910, respectively, Fig. 3c). The similar tendency was observed in the relationship between BW

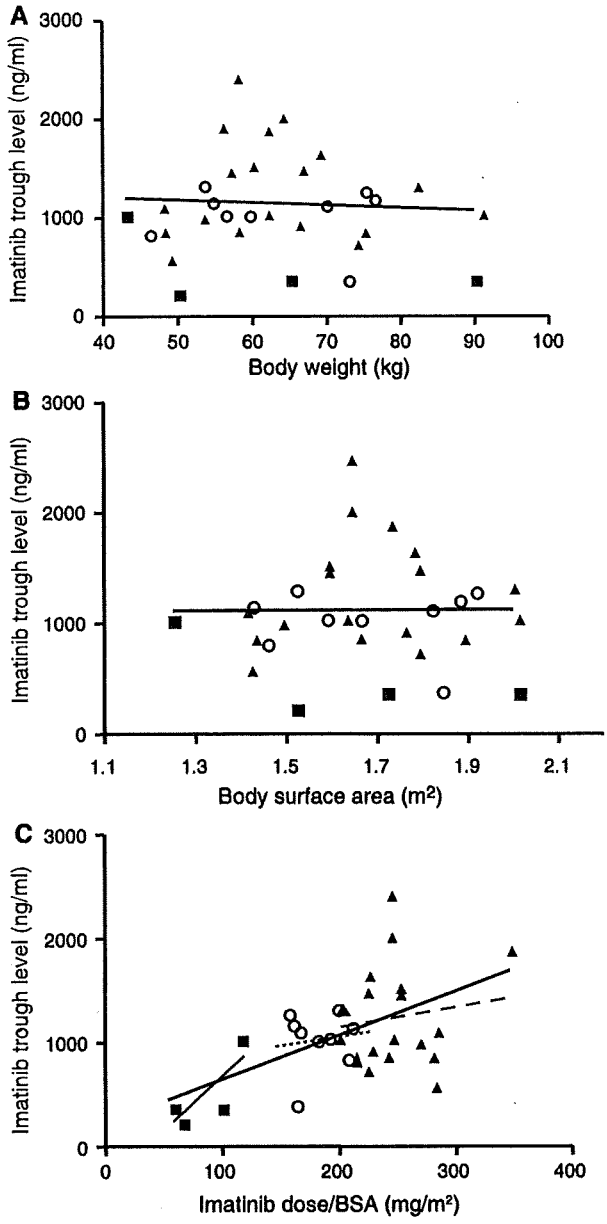

Fig. 3 Imatinib trough levels by body weight (**a**), body surface area, BSA (**b**), and daily imatinib dose divided by BSA (**c**). Imatinib trough and (**a**) body weight, $r^2 = 0.004$; **b** BSA, $r^2 < 0.001$; **c** imatinib dose/BSA, $r^2 = 0.28$. *Filled rectangles* represent cases taking imatinib 200 mg/day or less, *open circles* those taking 300 mg/day, *filled triangles* those taking 400 mg/day or more. *Bold line* represents a fit line in each figure. In **c**, *thin line* represents a fit line for those taking 200 mg/day or less, *dotted line* for those taking 300 mg/day, and *broken line* for those taking 400 mg/day or more. The imatinib trough level was significantly correlated with imatinib dose/BSA as total ($P = 0.0021$)

or BSA and imatinib concentration although not statistically significant (data not shown). There were eight out of thirteen patients (61.5%) whose imatinib concentration was higher than 1000 ng/ml despite taking 300 mg/day of imatinib or less. As shown in Fig. 4a, patients in the optimal-response category showed a significantly higher trough concentration than those in the suboptimal or failure categories ($P = 0.0087$). Similarly, 41% (10 out of 17) of the patients in the lower two quartiles (Q1 and Q2) and 94% (15 out of 16) in the upper two quartiles (Q3 and Q4) had an optimal response, demonstrating a significantly superior response (Table 3, $P = 0.04$) in the groups with a high-trough concentration. We also found a significant relationship between dose/BSA and the response ($P = 0.01$, Fig. 4b), and the dose and response ($P = 0.01$, Fig. 4c). These tendencies did not change even cases were divided into chronic and accelerated phases ($P = 0.0272$, Fig. 4d, e). Of note, there was no difference in the trough imatinib levels between patients with or without prior treatment (data not shown).

4 Discussion

We analyzed the long-term results of 73 CML patients initially treated with imatinib in a practical clinical setting, and confirmed its excellent long-term efficacy as in our previous report [7]. Despite administration of a lower dose of imatinib as compared to the IRIS study (400 mg/day of imatinib or more in 92% of patients), the OS and CCR of our patients were comparable to those observed in the IRIS study [6]. These results were surprising considering that our patients were older and in a more advanced stage (i.e., 12 out of 73 were not in the chronic phase at diagnosis) than those in the IRIS study. To address why smaller amount of imatinib could provide an excellent response for patients in the Nagasaki Study, we measured the trough concentration of imatinib and found that it was comparable or higher than those reported in foreign studies (mean = 1058 and 1119 ng/ml in the French and Nagasaki Study, respectively, median = 979 and 1040 ng/ml in the IRIS and Nagasaki study, respectively) [8, 9]. Although our results are based on a relatively small number of patients, the mean imatinib trough concentration of patients administered with 400 mg/day was higher in our analysis (1244 ± 494 ng/ml) than that reported from a French group study (1058 ± 557 ng/ml) [8]. The trough imatinib concentration had the strongest relationship with imatinib dose/BSA compared to that with body weight or BSA alone, which might explain the paradoxical median trough concentration in patients taking 300 mg/day (1130 ng/ml) or 400 mg/day (1040 ng/ml).

It was demonstrated that the trough concentration of imatinib relates to the cytogenetic and molecular responses from two different groups [8, 9]. In accordance with these reports, despite the possibility of inappropriate inclusion of late responders, the clinical and molecular efficacy of